

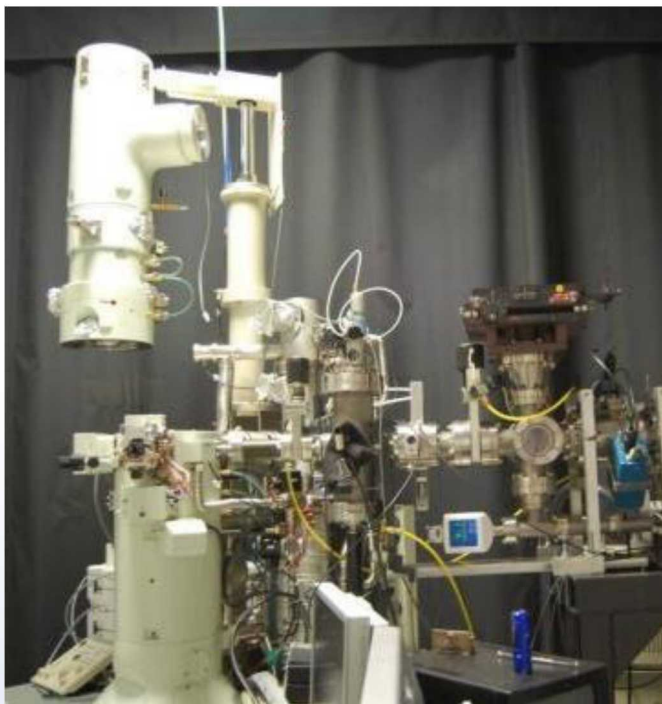
# Exploring the Response of Materials to Radiation with *In situ* Microscopy

SAND2016-9693PE

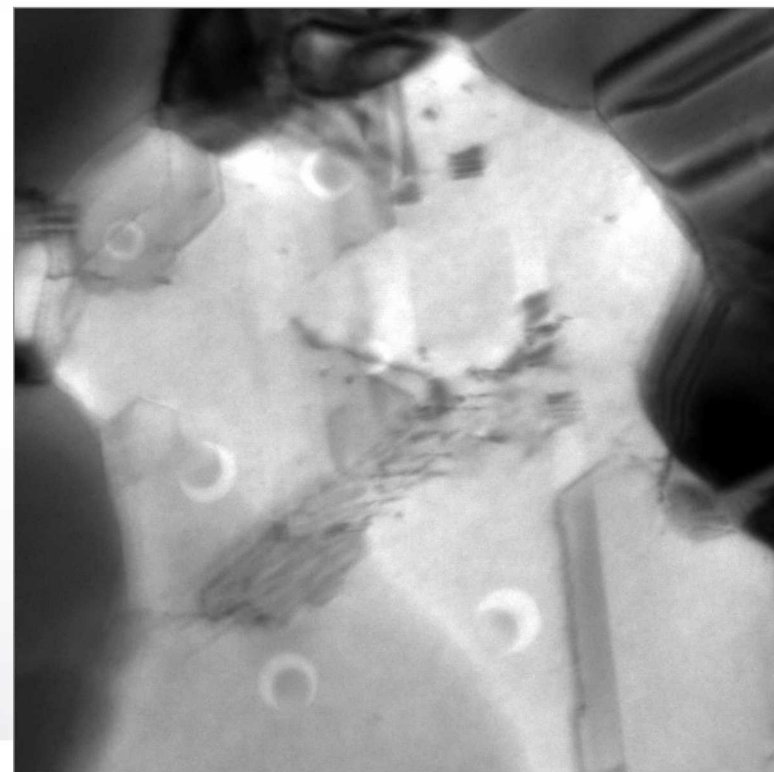
K. Hattar

Ion Beam Lab at Sandia National Laboratories

September 26, 2016



*In situ* TEM  
microscopy  
has recently  
undergone  
significant growth  
providing  
capabilities to  
investigate the  
structural evolution  
that occurs due to  
various extreme  
environments and  
combinations  
thereof

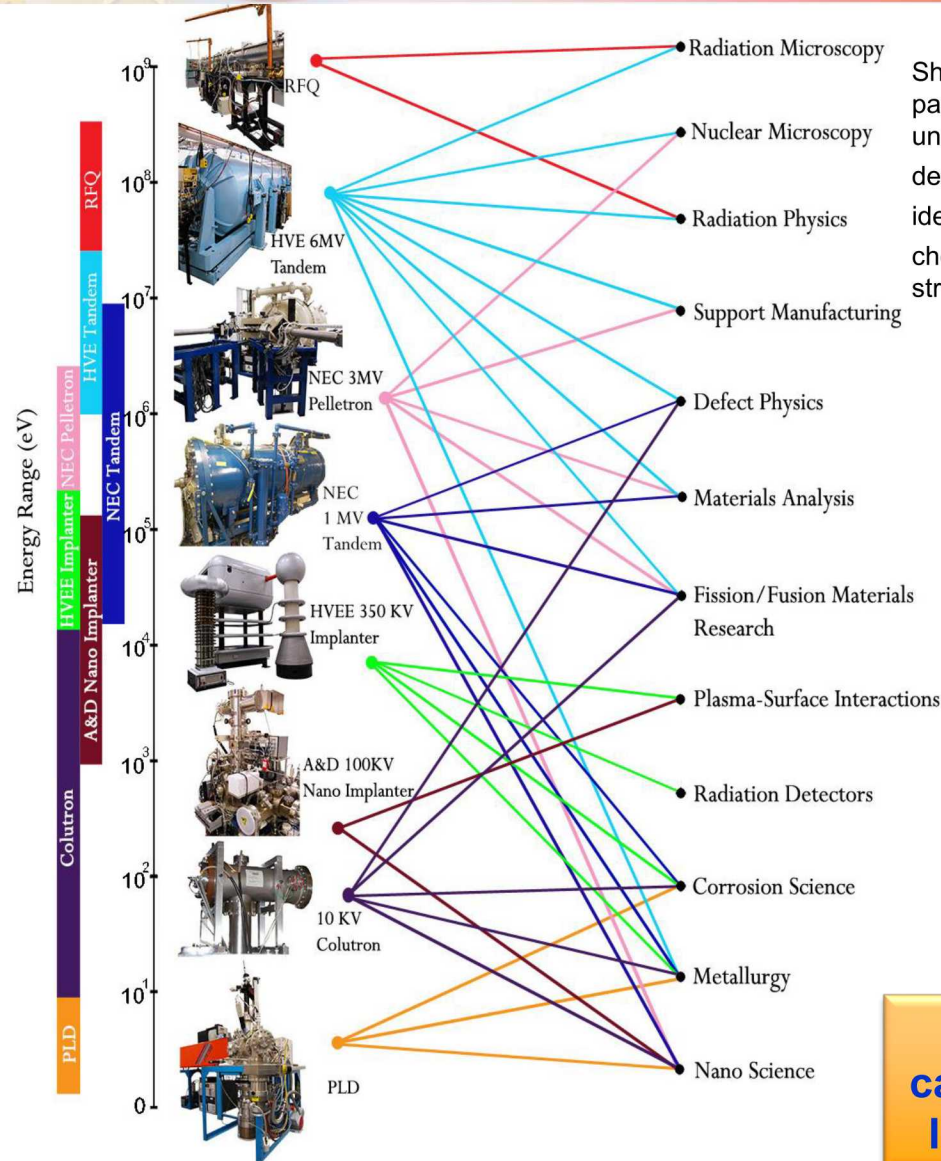


## Collaborators:

- IBL: D.C. Bufford, D. Buller, C. Chisholm, B.G. Clark, J. Villone, G. Vizkelethy, B.L. Doyle, S. H. Pratt, & M.T. Marshall
- Sandia: B. Boyce, T.J. Boyle, P.J. Cappillino, J.A. Scott, B.W. Jacobs, M.A. Hekmaty, D.B. Robinson, E. Carnes, J. Brinker, D. Sasaki, J.A. Sharon, T. Nenoff, W.M. Mook, B.R. Muntifering, P. Feng, F.P. Doty, B.A. Hernandez-Sanchez, P. Yang, J-E Mogonye, S.V. Prasad, P. Kotula, & C. Snow
- External: A. Minor, L.R. Parent, I. Arslan, H. Bei, E.P. George, P. Hosemann, D. Gross, J. Kacher, & I.M. Robertson

This work was supported by the US Department of Energy, Office of Basic Energy Sciences.

# Sandia's Ion Beam Laboratory

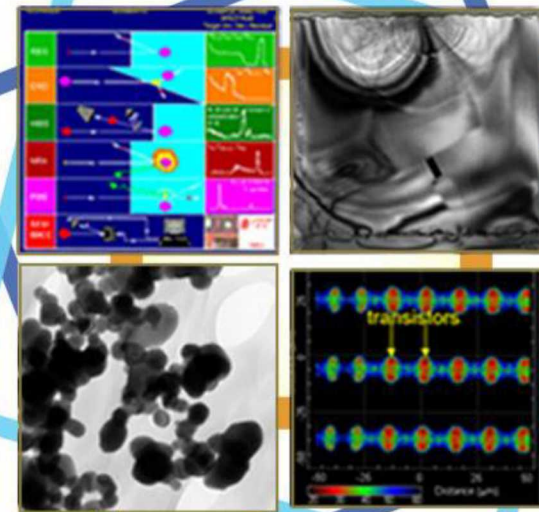


## Ion Beam Analysis (IBA)

Shooting a charged particle at an unknown material to determine its identity, local chemistry, and structure.

## Ion Beam Modification (IBM)

Changing the optical, mechanical, and chemical properties of materials via ion implantation to meet technological needs



## In Situ Ion Irradiation Microscopy (I<sup>3</sup>M)

Bombarding nano samples with various particles and observing the changes in real time to understand how materials will behave in extreme environments.

## Radiation Effects Microscopy (REM)

Using ion emissions to determine the Radiation hardness of microelectronics, identifying potential weaknesses.

**The IBL has a unique and comprehensive capability ion beam set including and *In situ* Ion Irradiation Transmission Electron Microscopy.**

# Benefits & Limitations of *in situ* TEM

## Benefits

1. Real-time nanoscale resolution observations of microstructural dynamics

## Limitations

1. Predominantly limited to microstructural characterization
  - Some work in thermal, optical, and mechanical properties
2. Limited to electron transparent films
  - Can often prefer surface mechanisms to bulk mechanisms
  - Local stresses state in the sample is difficult to predict
3. Electron beam effects
  - Radiolysis and Knock-on Damage
4. Vacuum conditions
  - $10^{-7}$  Torr limits gas and liquid experiments feasibility
5. Local probing
  - Portions of the world study is small

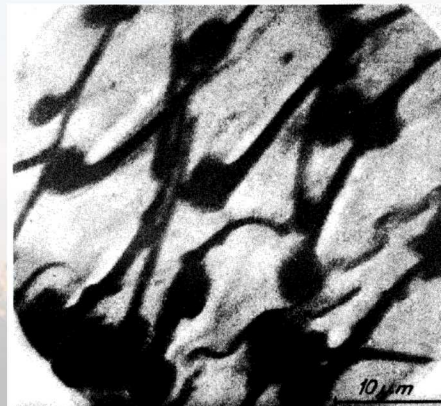


Fig. 6: Wing surface of the house fly:  
(First internal photography,  $U = 60$  kV,  $M_s = 2200$ )  
(Driest, E., and Müller, H.O. Z. Wiss. Mikroskope 52, 53-57 (1955))

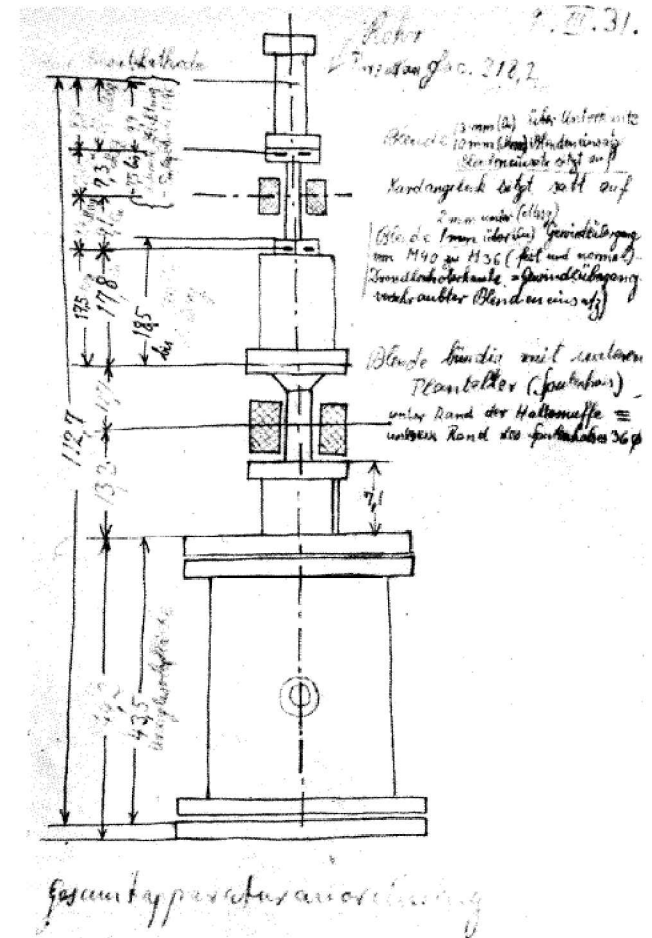


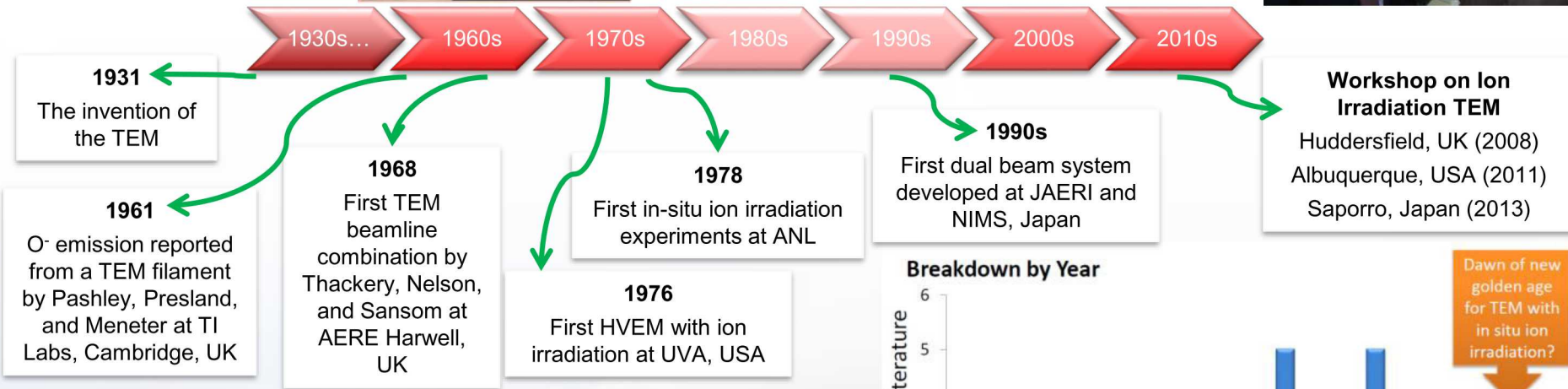
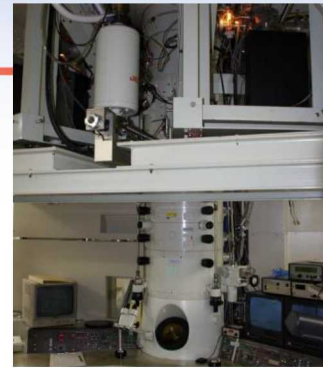
Fig. 2: Sketch by the author (9 March 1931) of the cathode ray tube for testing one-stage and two-stage electron-optical imaging by means of two magnetic electron lenses (electron microscope) [8].



# History of *In situ* Ion Irradiation TEM



Courtesy of: J. Hinks

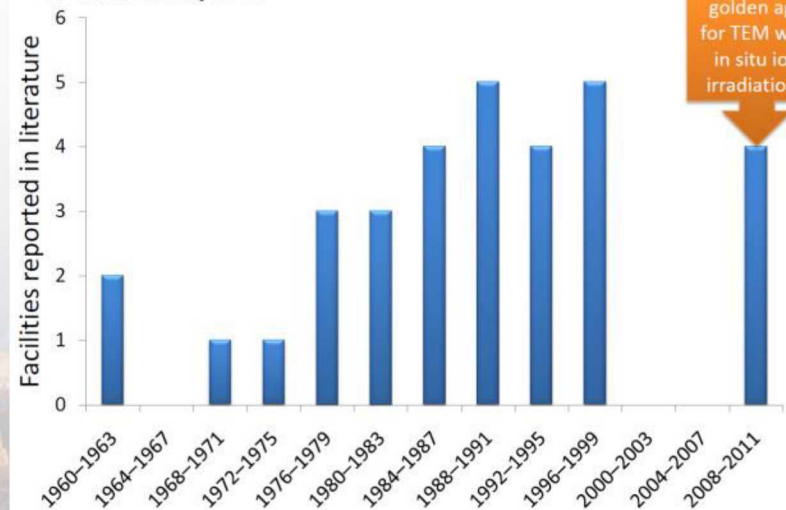


**“The direct observation of ion damage in the electron microscope thus represents a powerful means of studying radiation damage”**



D.W. Pashley and A.E.B. Presland Phil Mag. 6(68) 1961 p. 1003

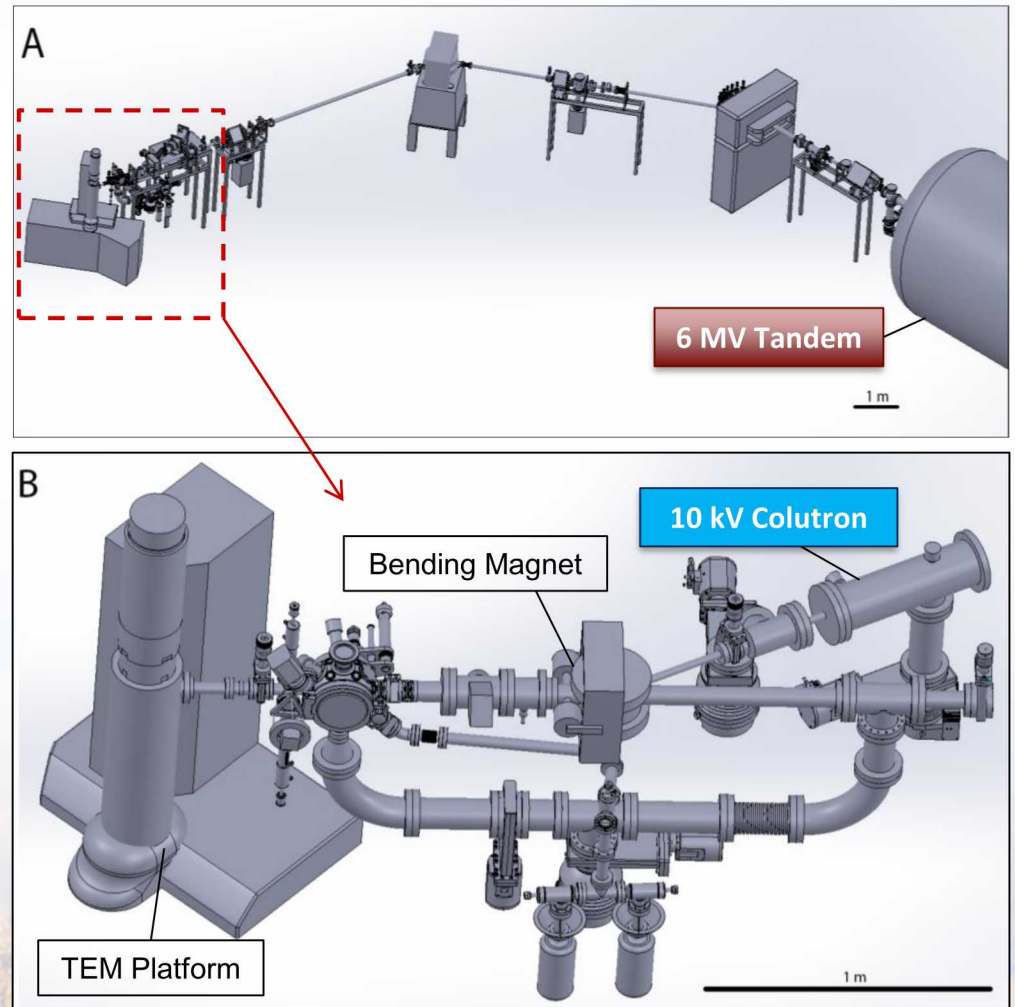
**Breakdown by Year**



# *In situ* Ion Irradiation TEM Facility

## Proposed Capabilities

- 200 kV LaB<sub>6</sub> TEM
- Ion beams considered:
  - Range of Sputtered Ions
  - 10 keV D<sup>2+</sup>
  - 10 keV He<sup>+</sup>
- All beams hit same location
- Nanosecond time resolution (DTEM)
- Precession scanning (EBSD in TEM)
- *In situ* PL, CL, and IBIL
- *In situ* vapor phase stage
- *In situ* liquid mixing stage
- *In situ* heating
- Tomography stage (2x)
- *In situ* cooling stage
- *In situ* electrical bias stage
- *In situ* straining stage



Solid Works by: J. Davis



# Planned Development of the I<sup>3</sup>TEM

Collaborators: D.L. Buller, B.G. Clark, D. Masiel, & B.L. Doyle

## 0<sup>th</sup> Generation

- 200 kV LaB<sub>6</sub> TEM
- *In situ* vapor phase stage
- *In situ* liquid mixing stage
- Simple tomography holder

## 1<sup>st</sup> Generation

- Insertion of collimated Tandem ion beam at 0-9°
- Vacuum, electrical, and mechanical Isolation
- Adequate dosimetry

## 2<sup>nd</sup> Generation

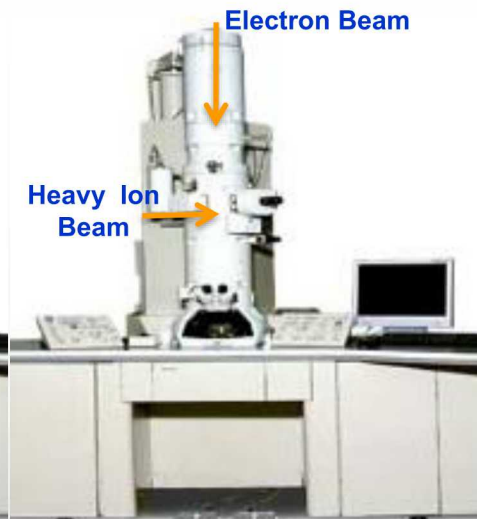
- Concurrent heavy and light ion implantation
- A Colutron ion beam will be bent in line with the Tandem beam.

## 3<sup>rd</sup> Generation

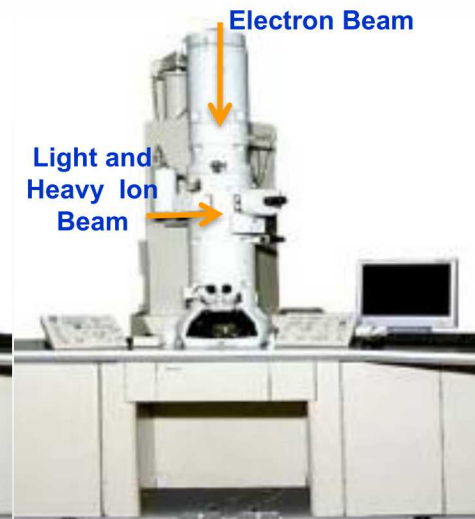
- Plan-view laser exposure and DTEM capabilities
- Provide ion and laser excitation sources with nanosecond timing



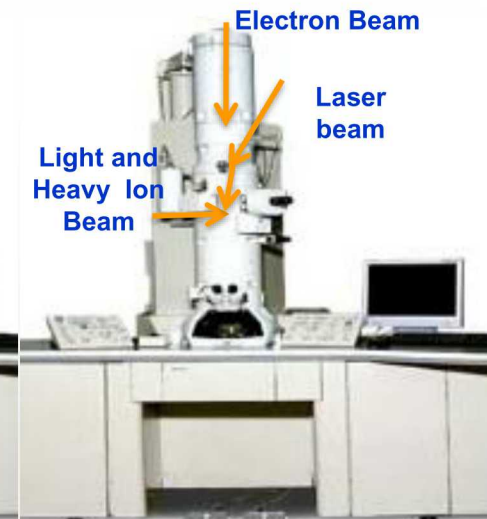
Delivery October 29, 2010 &  
Accepted January 31, 2011



First Tandem beam into TEM  
April 19, 2011



First Colutron beam into TEM  
October 3, 2012



Optical port completed  
Laser optics are being designed

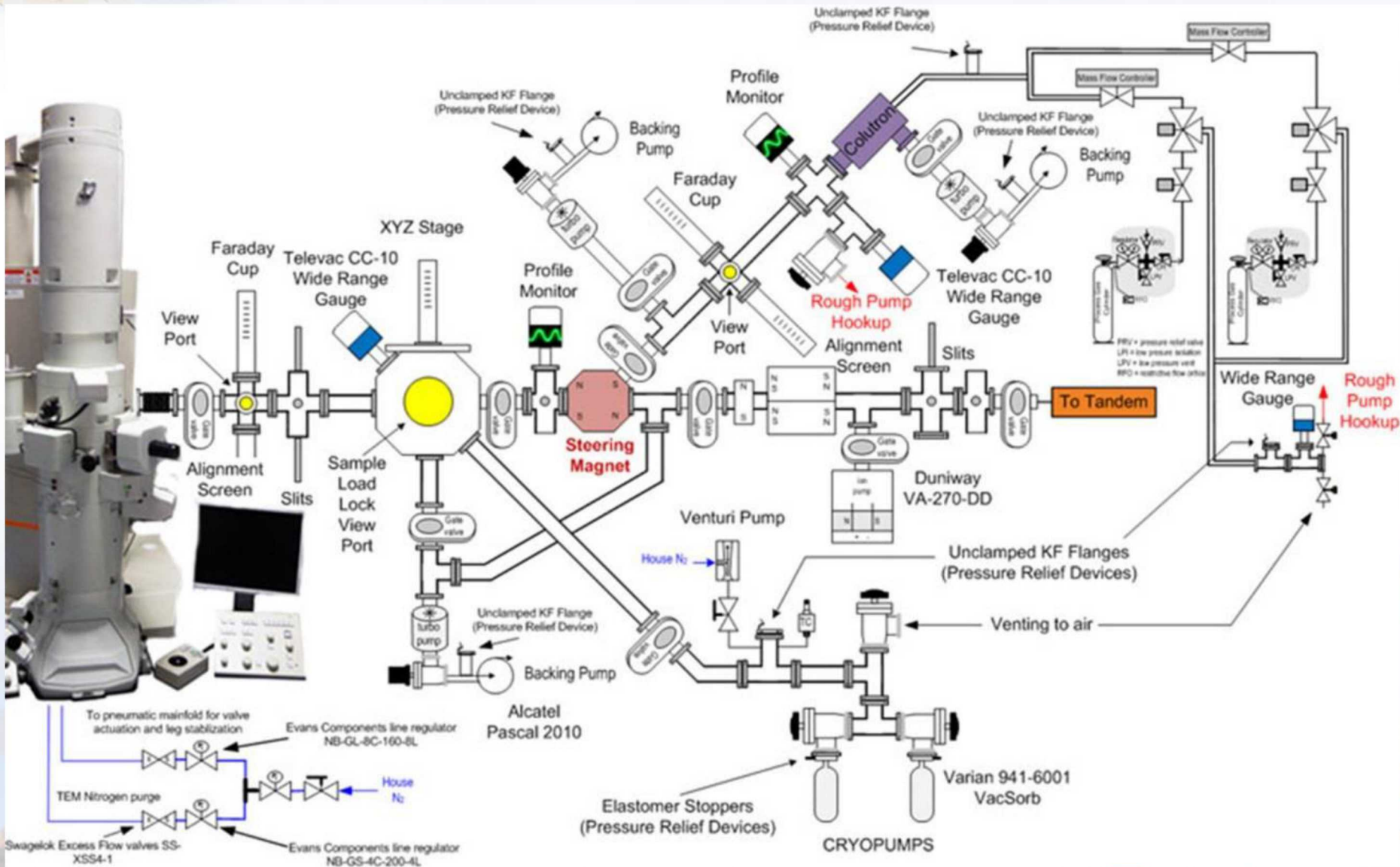
Each facility addition will expand potential capabilities



Sandia National Laboratories

# Schematic of the *In situ* TEM Beamline

Collaborators: M.T. Marshall J.A. Scott, & D.L. Buller



# TEM Facility

Collaborators: D.L. Buller & J.A. Scott

200 keV JEOL-2100

Stages:

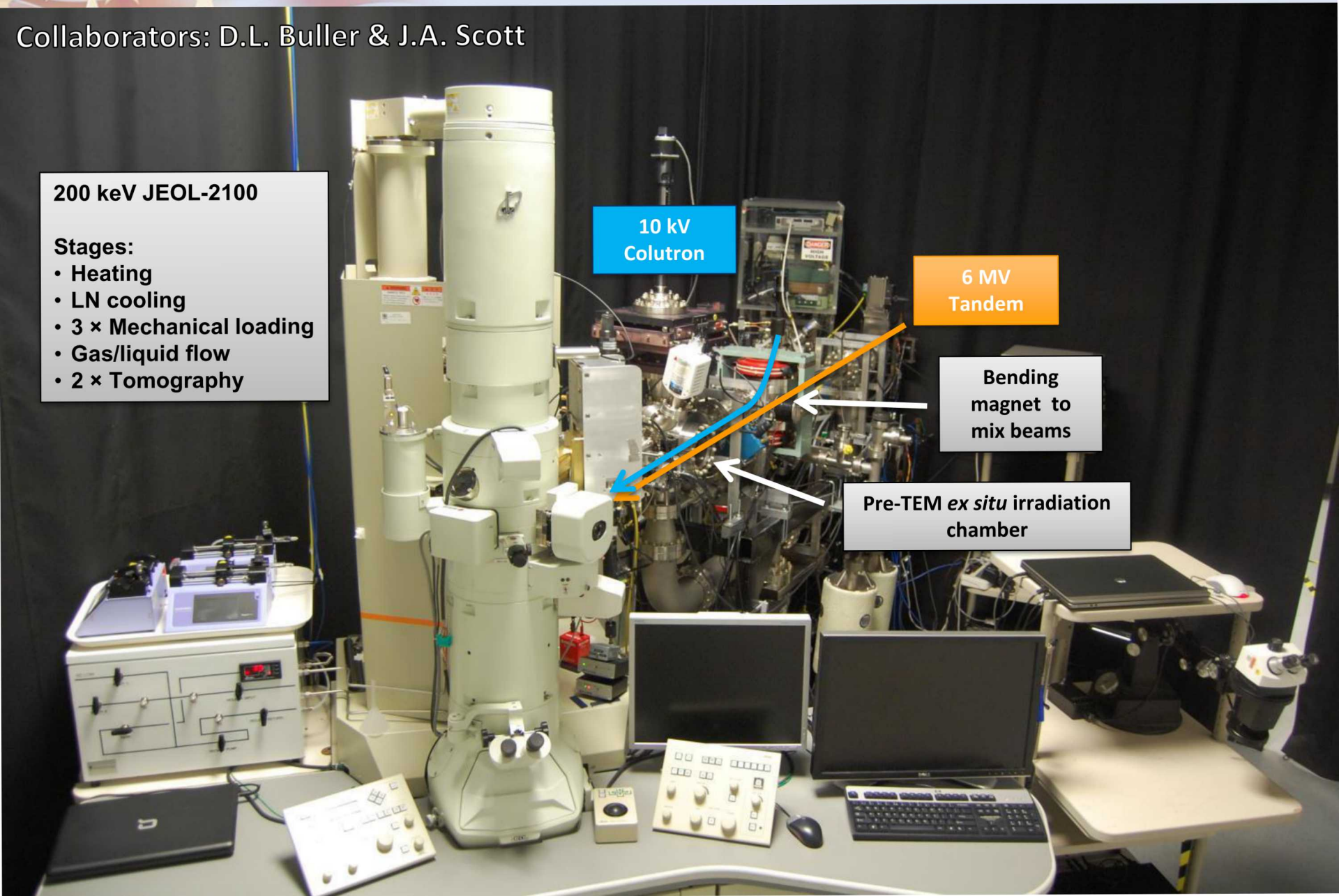
- Heating
- LN cooling
- 3 × Mechanical loading
- Gas/liquid flow
- 2 × Tomography

10 kV  
Colutron

6 MV  
Tandem

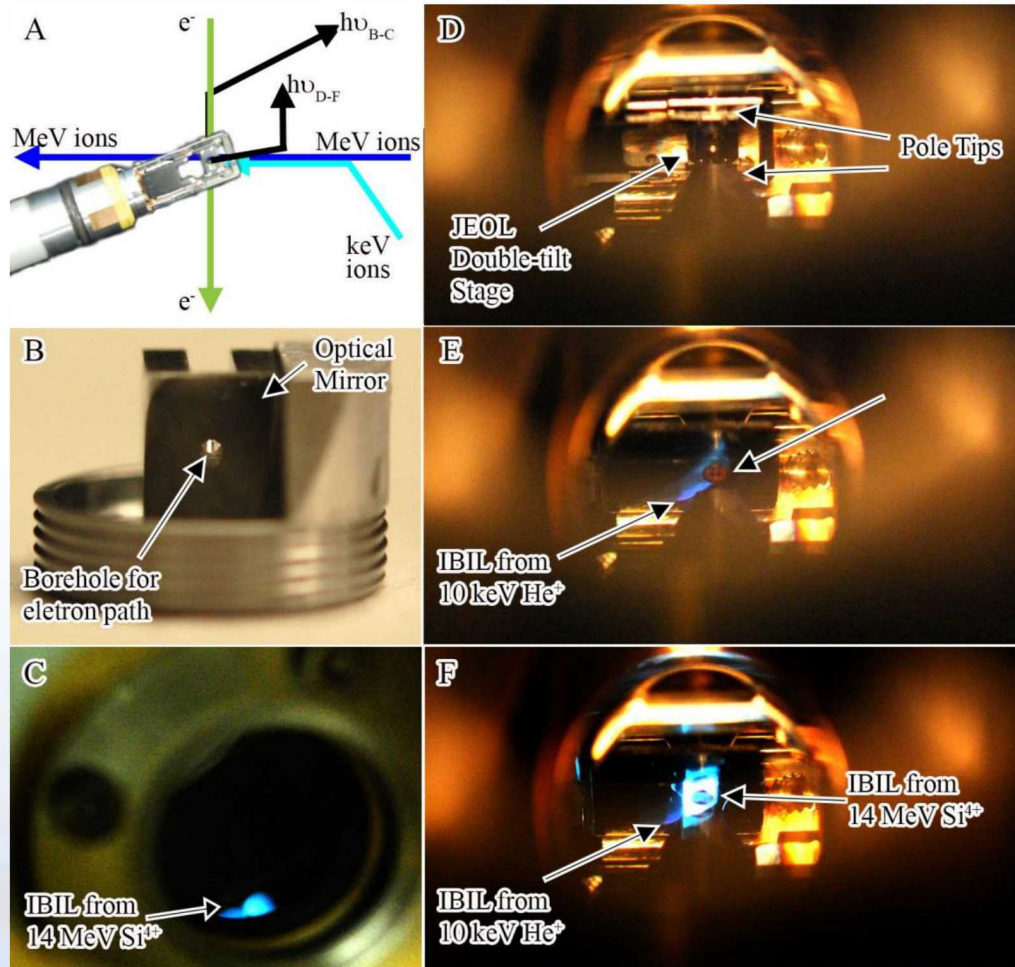
Bending  
magnet to  
mix beams

Pre-TEM *ex situ* irradiation  
chamber



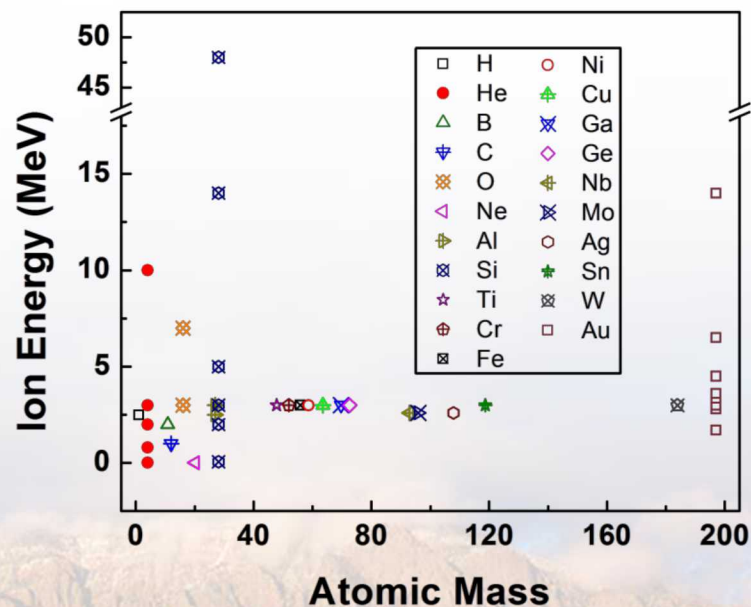
# Visualizing Ion Beams in the TEM

## IBIL from a quartz stage inside the TEM



**Ion beam alignment at the sample confirmed using ion beam-induced luminescence**

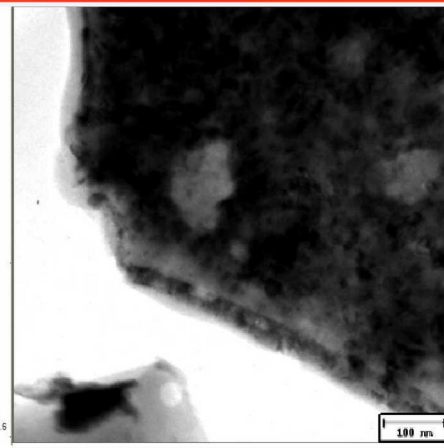
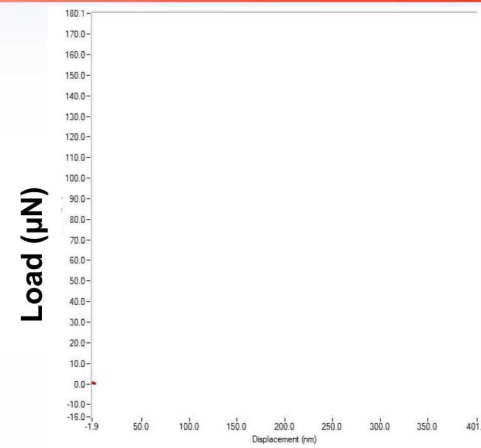
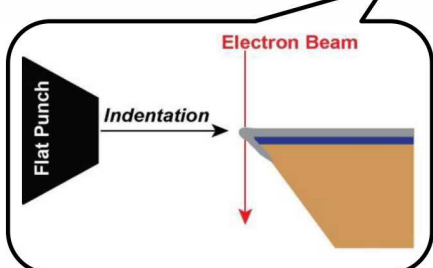
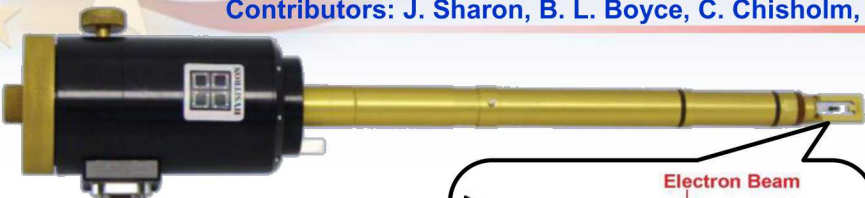
## Ion species & energy introduced into the TEM



Hattar, et al, under review 2014.

# Next Steps: *In situ* TEM Quantitative Mechanical Testing

Contributors: J. Sharon, B. L. Boyce, C. Chisholm, H. Bei, E.P. George, P. Hosemann, A.M. Minor, & Hysitron Inc.

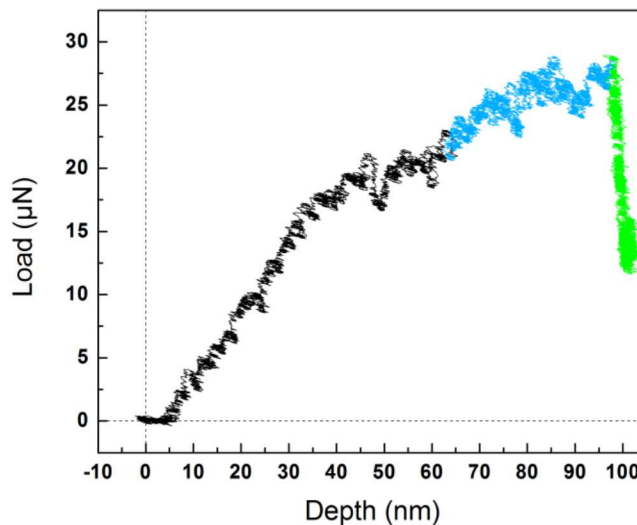
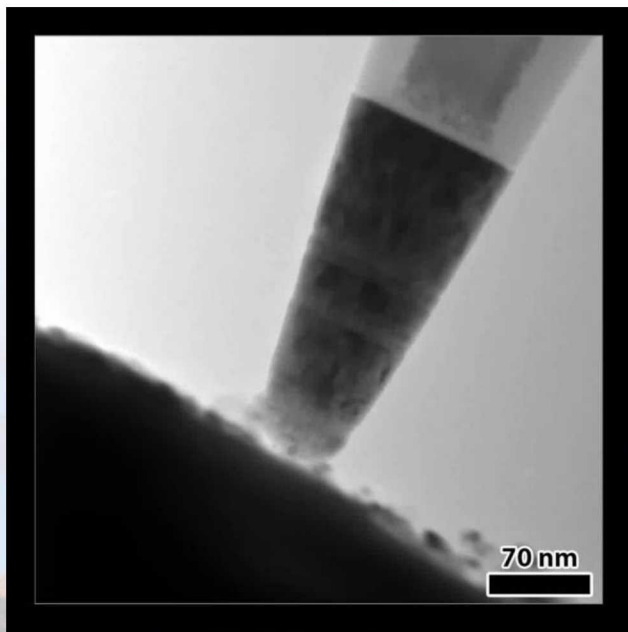


## Range of Mechanical Testing Techniques

- Indentation
- Tension
- Fatigue
- Compression
- Wear
- Creep

Displacement (nm)

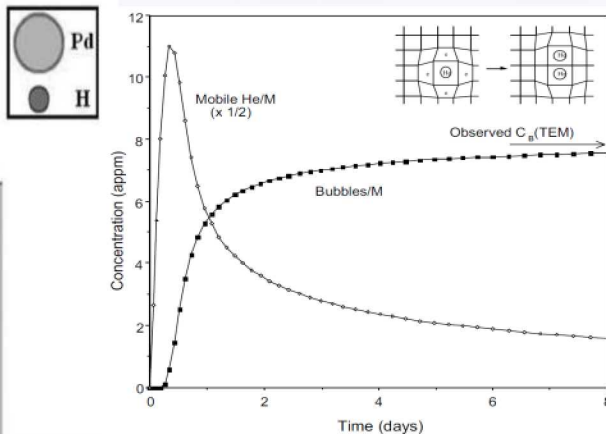
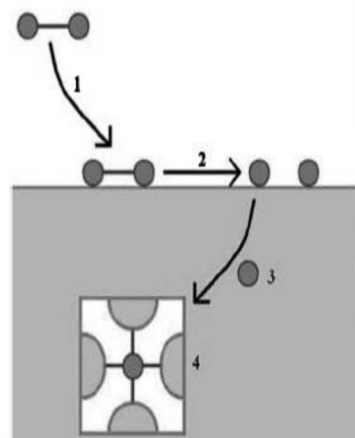
## Fundamentals of Mechanical Properties



- 0.5 nm/s loading rate
- Trapezoid load function
- 60s load/60s hold/60s unload

# Can *In situ* TEM Address Hydrogen Storage Concerns in Extreme Environments?

Contributors: B.G. Clark, P.J. Cappillino, B.W. Jacobs, M.A. Hekmaty, D.B. Robinson, L.R. Parent, I. Arslan. & Protochips, Inc.



R. Delmelle, J., Phys. Chem. Chem. Phys. (2011) p.11412

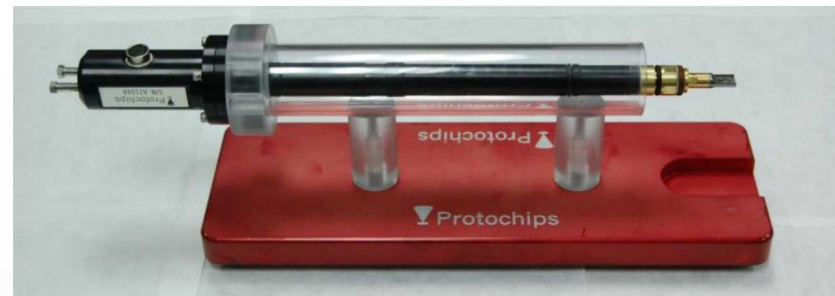
Cowgill, D., Fusion Sci. & Tech., 28 (2005) p. 539

Trinkaush, H. et al., JNM (2003) p. 229

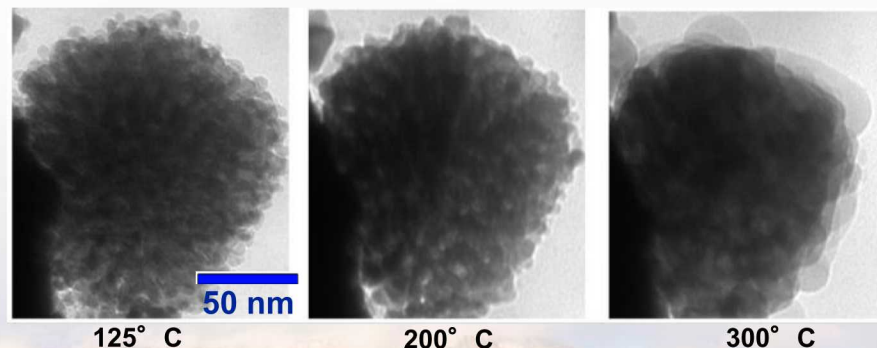
Thiebaut, S. et al. JNM (2000) p. 217

## Vapor-Phase Heating TEM Stage

- Compatible with a range of gases
- In situ* resistive heating
- Continuous observation of the reaction channel
- Chamber dimensions are controllable
- Compatible with MS and other analytical tools

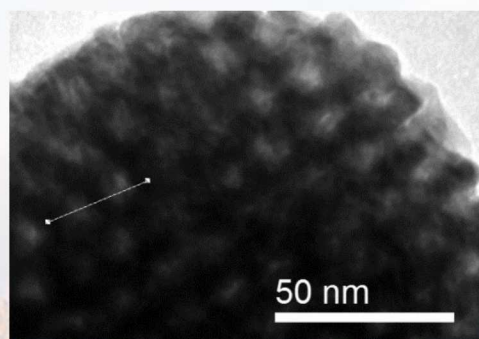
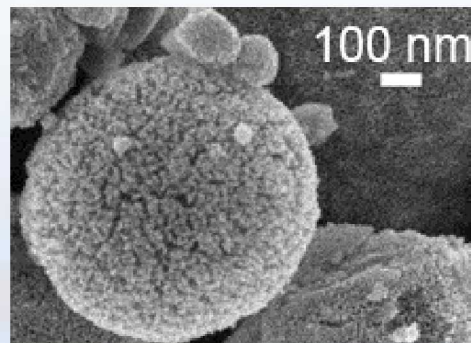


- 1 atm H<sub>2</sub> after several pulses to specified temp.



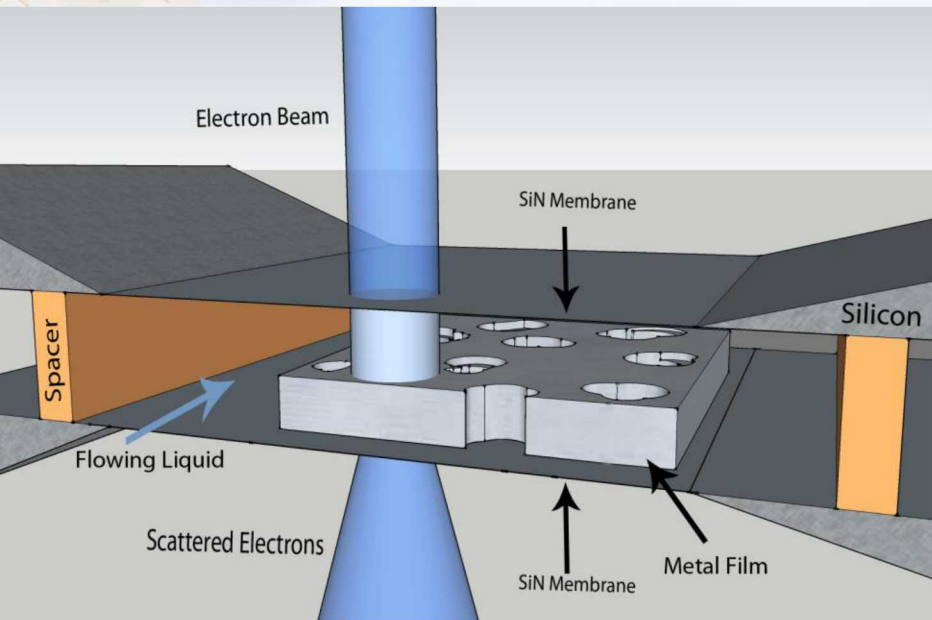
New *in situ* atmospheric heating experiments provide great insight into nanoporous Pd stability

Harmful effects may be mitigated in nanoporous Pd



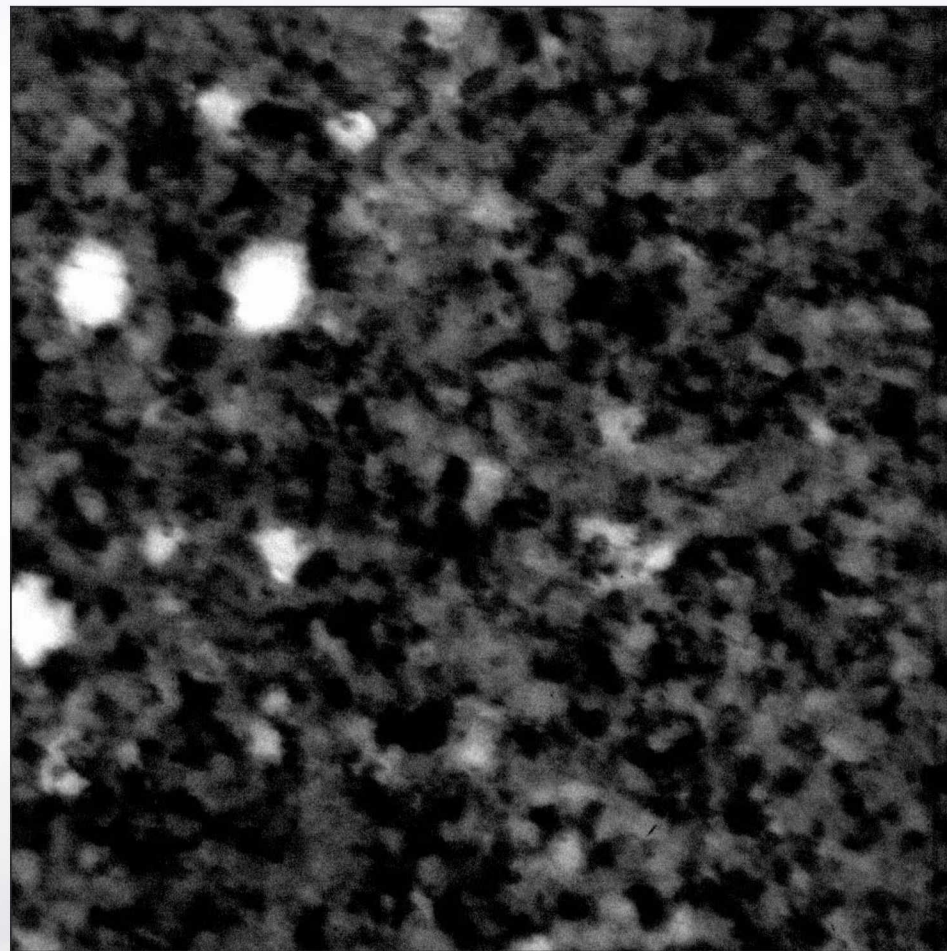
# *In situ* TEM Corrosion

Contributors: D. Gross, J. Kacher, & I.M. Robertson



## Microfluidic Stage

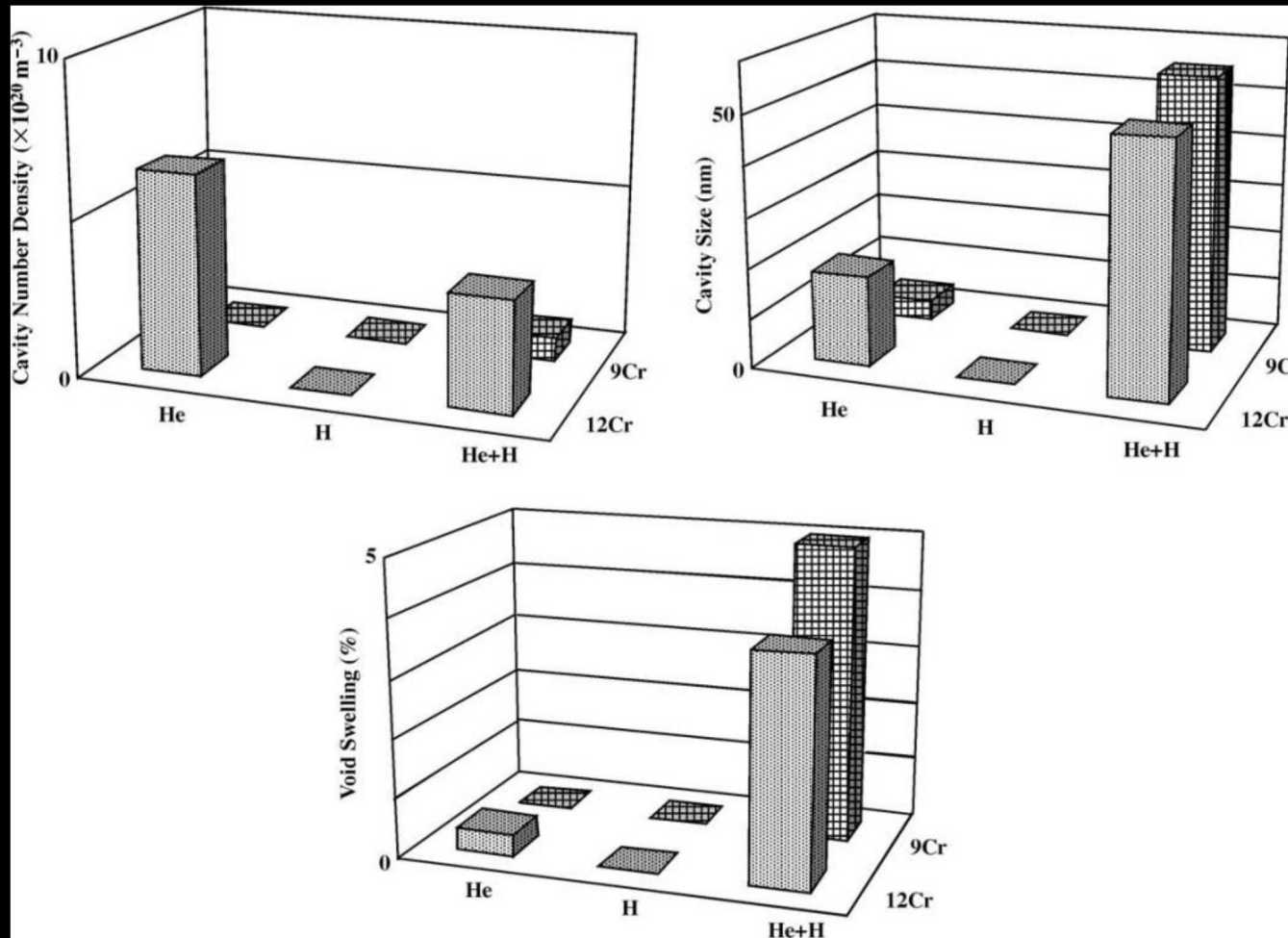
- Mixing of two or more channels
- Continuous observation of the reaction channel
- Chamber dimensions are controllable
- Films can be directly deposited on the electron transparent SiN membrane



**Pitting mechanisms during dilute flow of acetic acid over 99.95% nc-PLD Fe involves many grains.**



# H, He, and Displacement Damage Synergy



T. Tanaka et al. "Synergistic effect of helium and hydrogen for defect evolution under milt-ion irradiation of Fe-Cr ferritic alloys"

J. of Nuclear Materials 329-333 (2004) 294-298

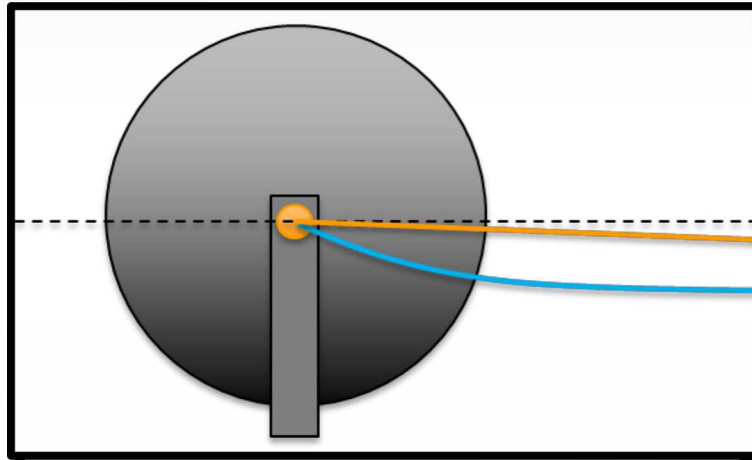
## Coupling Effect

- H and He are produced as decay products
- The relationship between the point defects present, the interstitial hydrogen, and the He bubbles in the system that results in the increased void swelling has only been theorized.
- The mechanisms which governs the increased void swelling under the presence of He and H have never been experimental determined

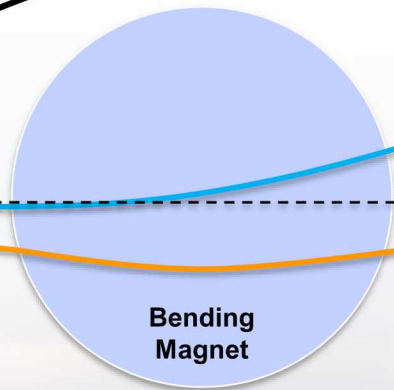
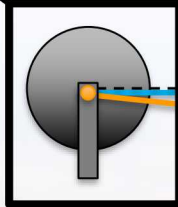
Difficulty of performing triple-beam irradiation has resulted in a limited number of facilities world wide

# Modeling Beam Mixing and Deflection

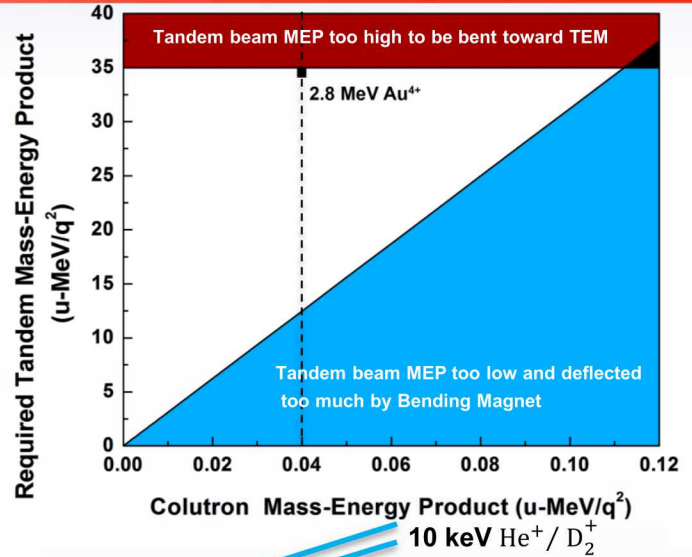
Collaborators: M. Steckbeck, D.C. Bufford, & B.L. Doyle



TEM  
Obj. Lens



Bending  
Magnet



Colutron Mass-Energy Product (u-MeV/q<sup>2</sup>)  
10 keV He<sup>+</sup> / D<sub>2</sub><sup>+</sup>

Steering Magnet

20°

2.8 MeV Au<sup>4+</sup>

- Must compensate for deflection of Tandem beam by bending magnet  
Colutron beams deflected by the TEM objective lens
- Insignificant deflection of Tandem beams
- With 10 keV He/D<sub>2</sub> we can use Tandem beams  $\approx 13$  MeV/q<sup>2</sup>
- Au, He, and D<sub>2</sub> ions all reach the sample concurrently

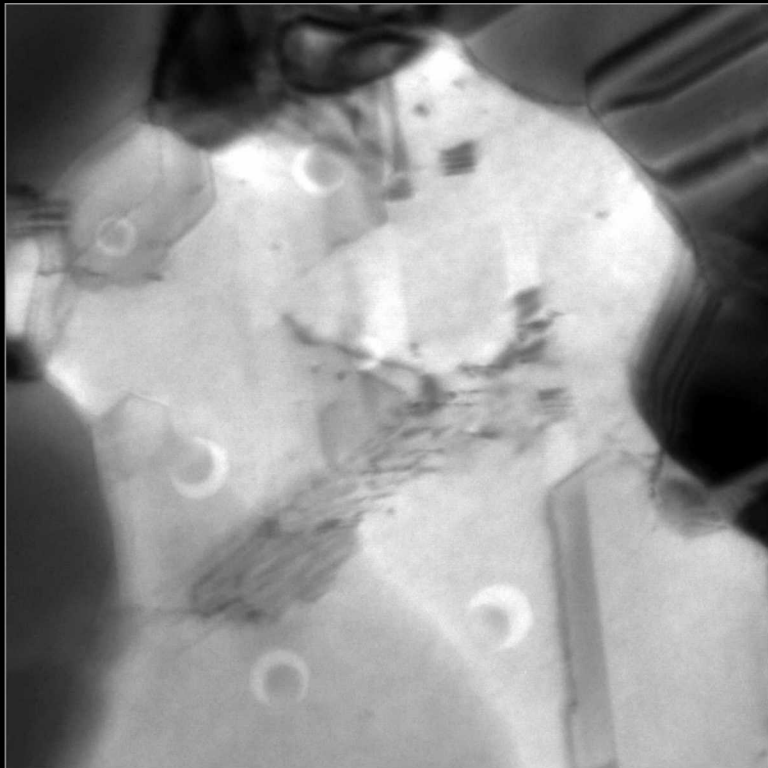


Sandia National Laboratories

# Single Ion Strikes

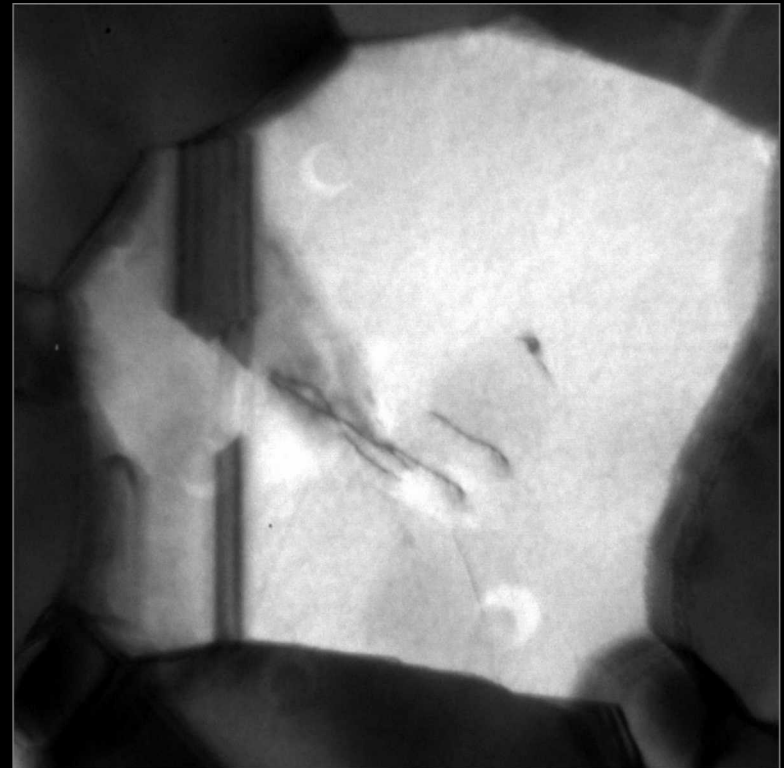
Collaborators: C. Chisholm , P. Hosemann, & A. Minor

$7.9 \times 10^9$  ions/cm<sup>2</sup>/s



**VS**

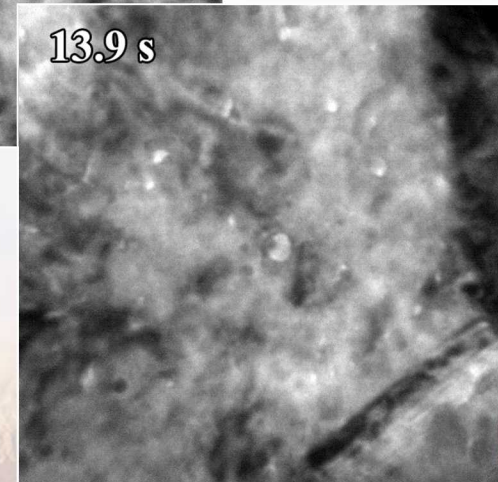
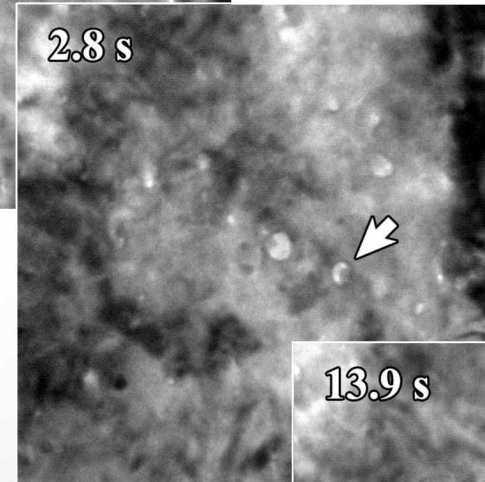
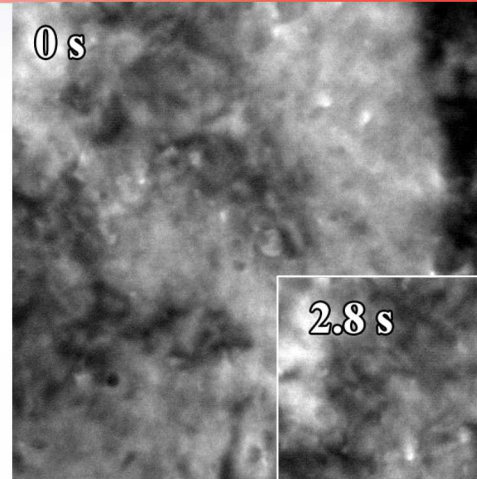
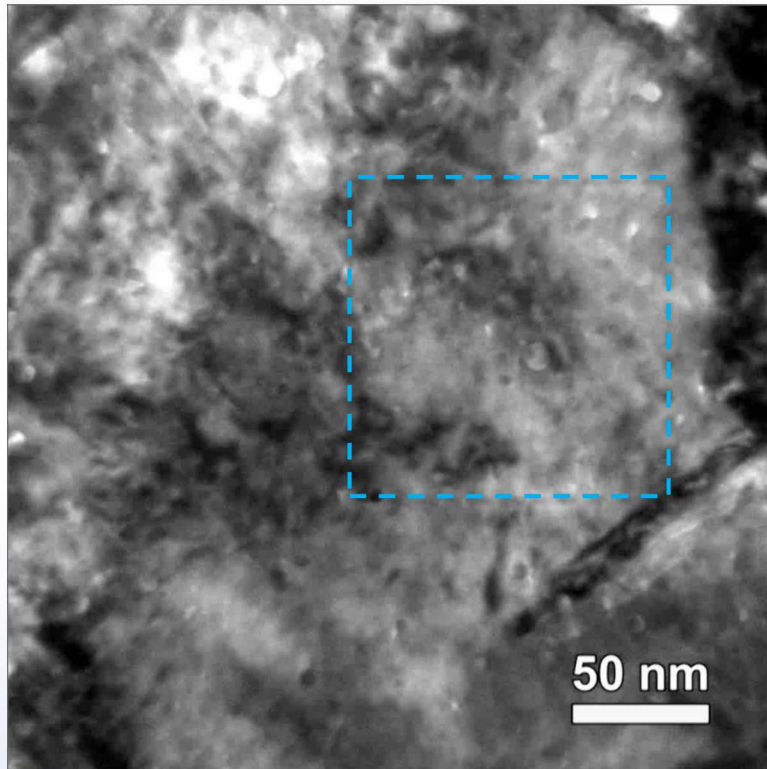
$6.7 \times 10^7$  ions/cm<sup>2</sup>/s



Improved vibrational and ion beam stability permits us to work at 120kx or higher permitting imaging of single cascade events

# 2.8 MeV Au<sup>4+</sup> + 10 keV He<sup>+</sup> / D<sub>2</sub><sup>+</sup>

Video playback speed x1.5.



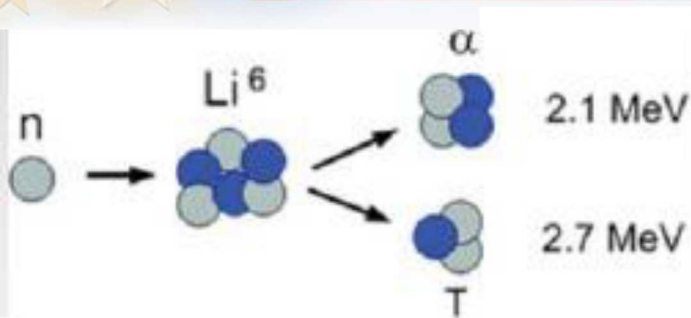
## ■ Approximate fluence:

- Au  $1.2 \times 10^{13}$  ions/cm<sup>2</sup>
- He  $1.3 \times 10^{15}$  ions/cm<sup>2</sup>
- D  $2.2 \times 10^{15}$  ions/cm<sup>2</sup>

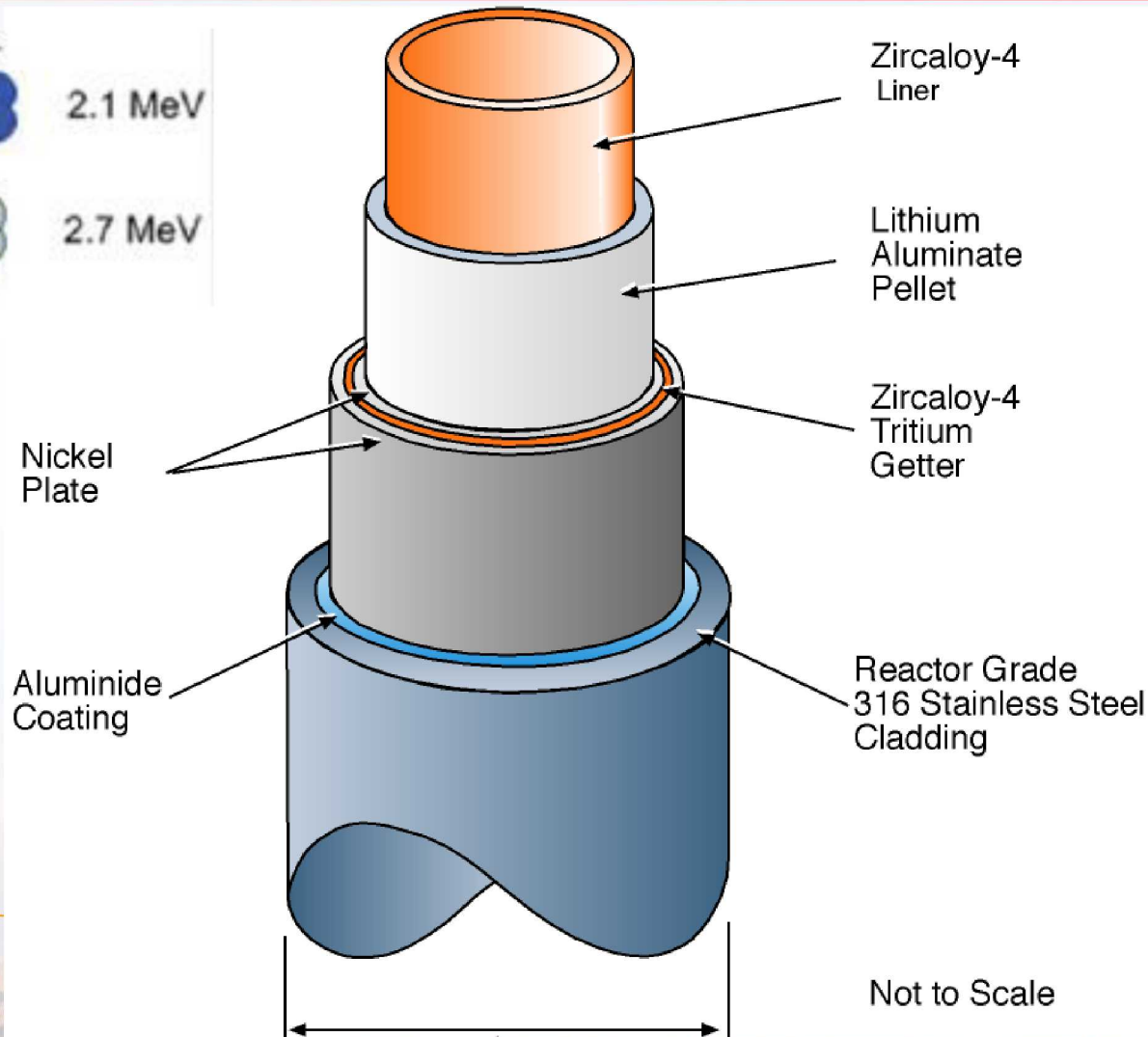
## ■ Cavity nucleation and disappearance



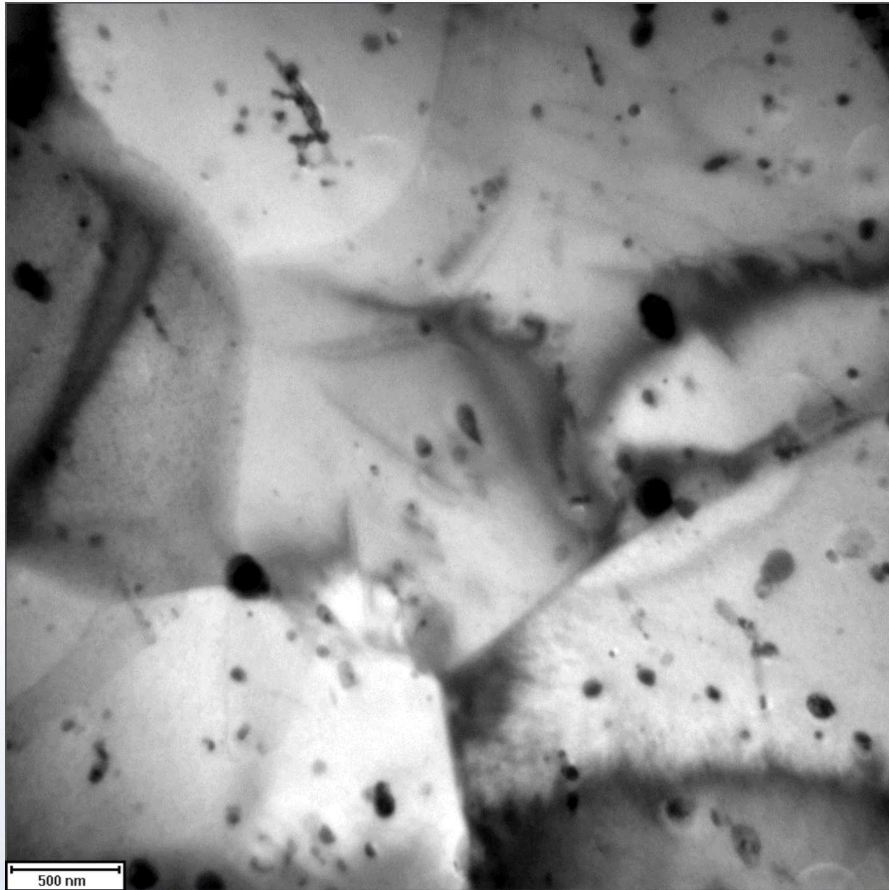
# Tritium Producing Burnable Absorber Rod (TPBAR)



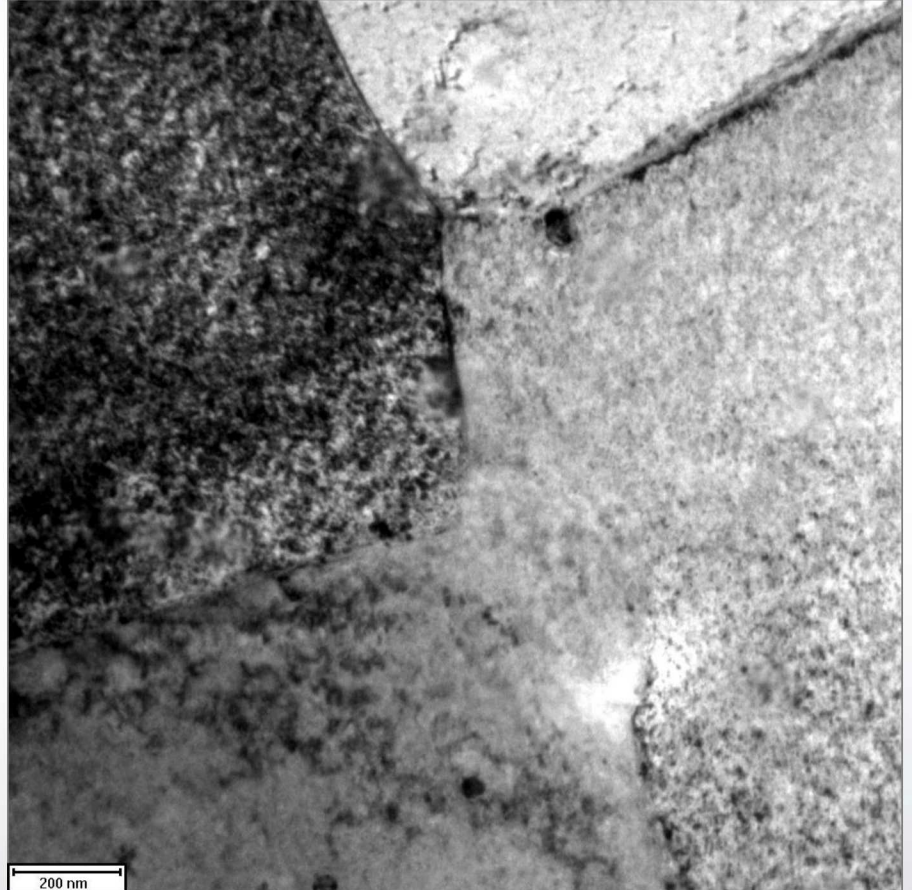
- Displacement Damage
- Helium Implantation
- Tritium Implantation
- Elevated Temperatures



# 3 MeV Self Ion Irradiation at 310 C



Before Irradiation

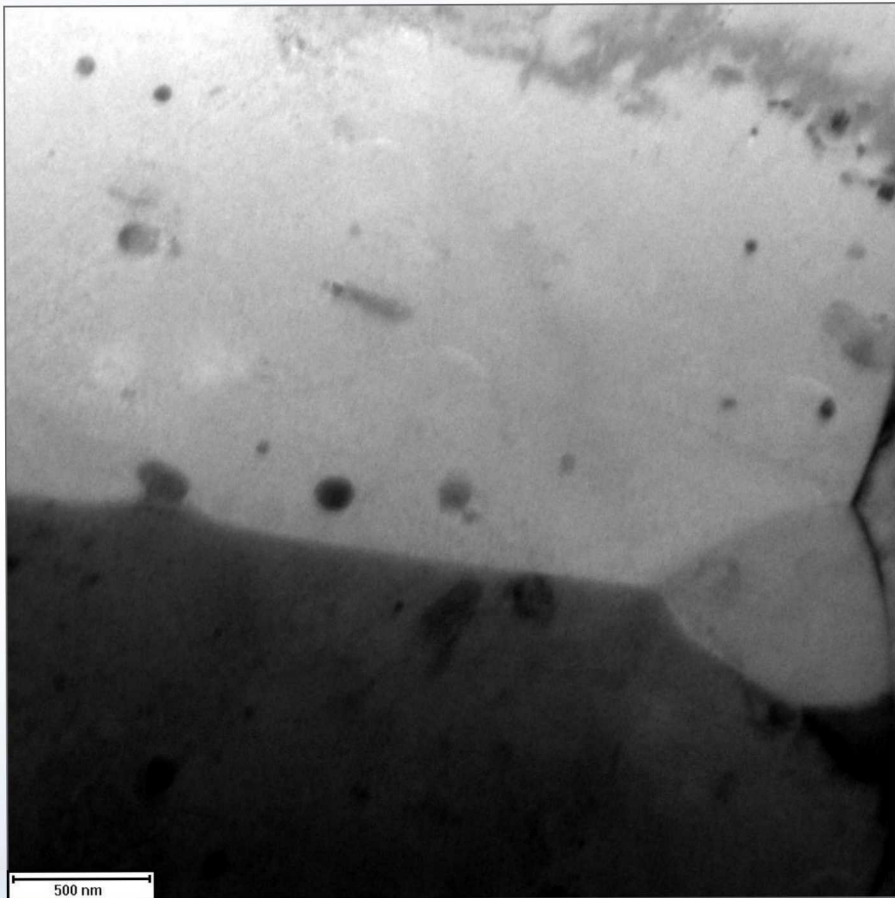


After Irradiation

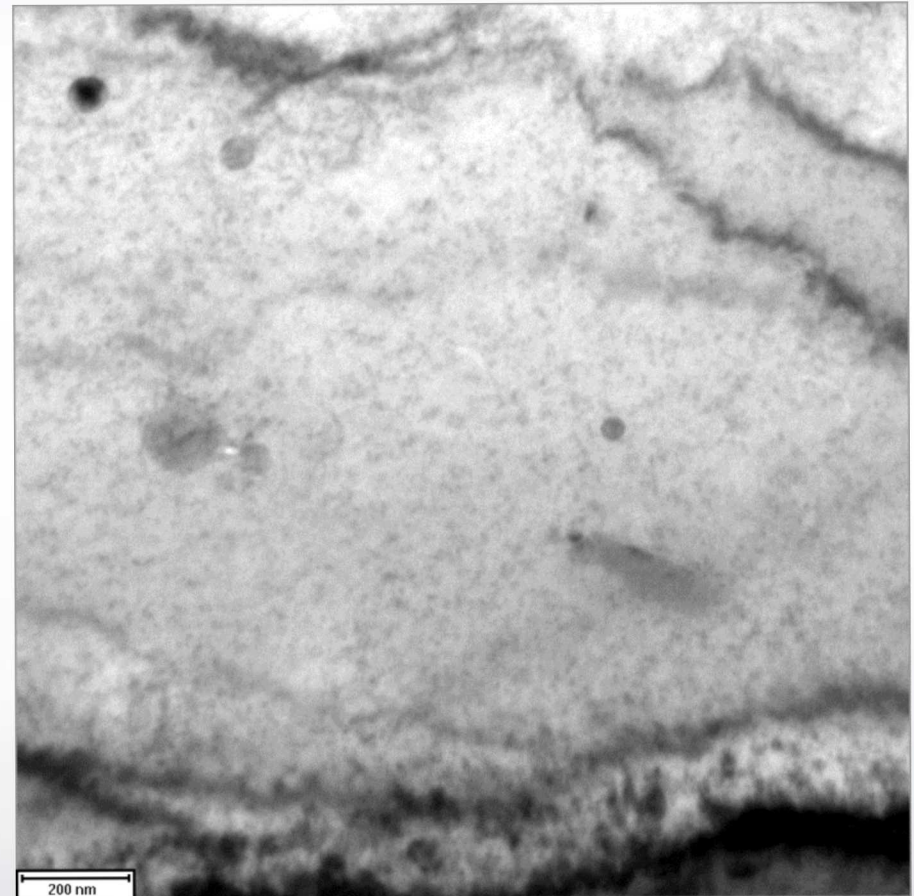
≈ 7 DPA



# 10 keV He<sup>+</sup> Implantation at 310 C

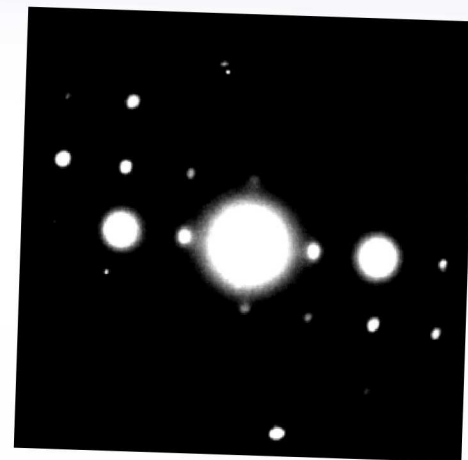


Before Implantation



After Implantation  
Damage, No Cavities

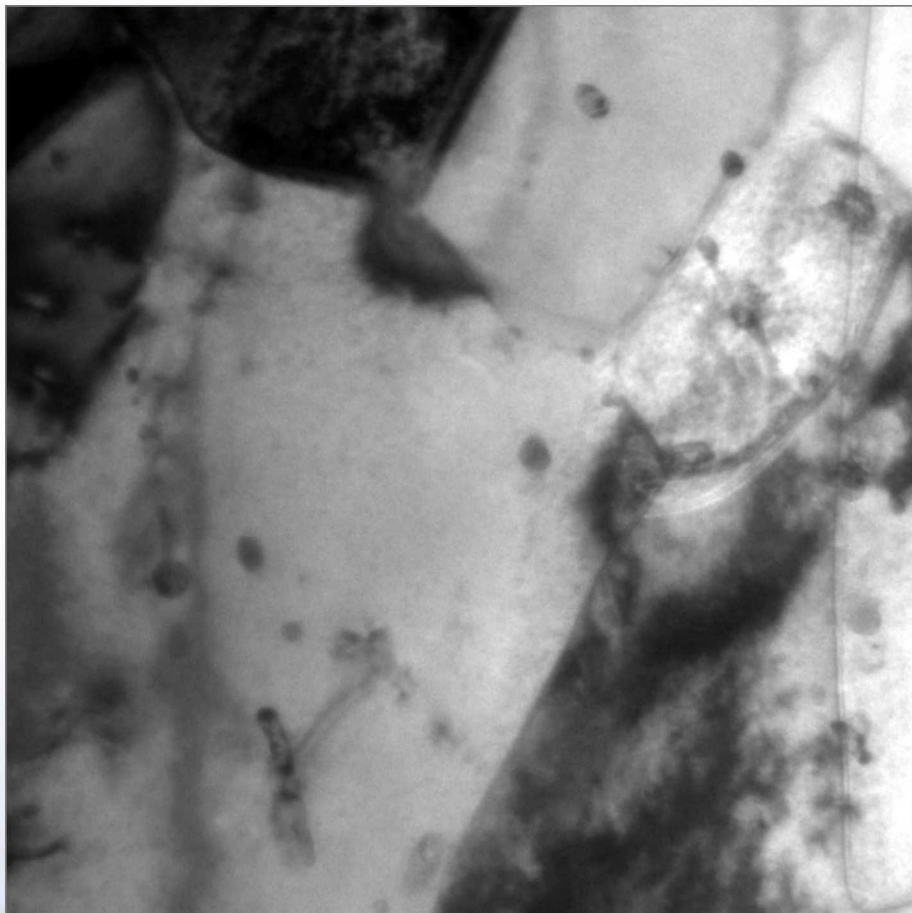
# He<sup>+</sup> Followed by Zr



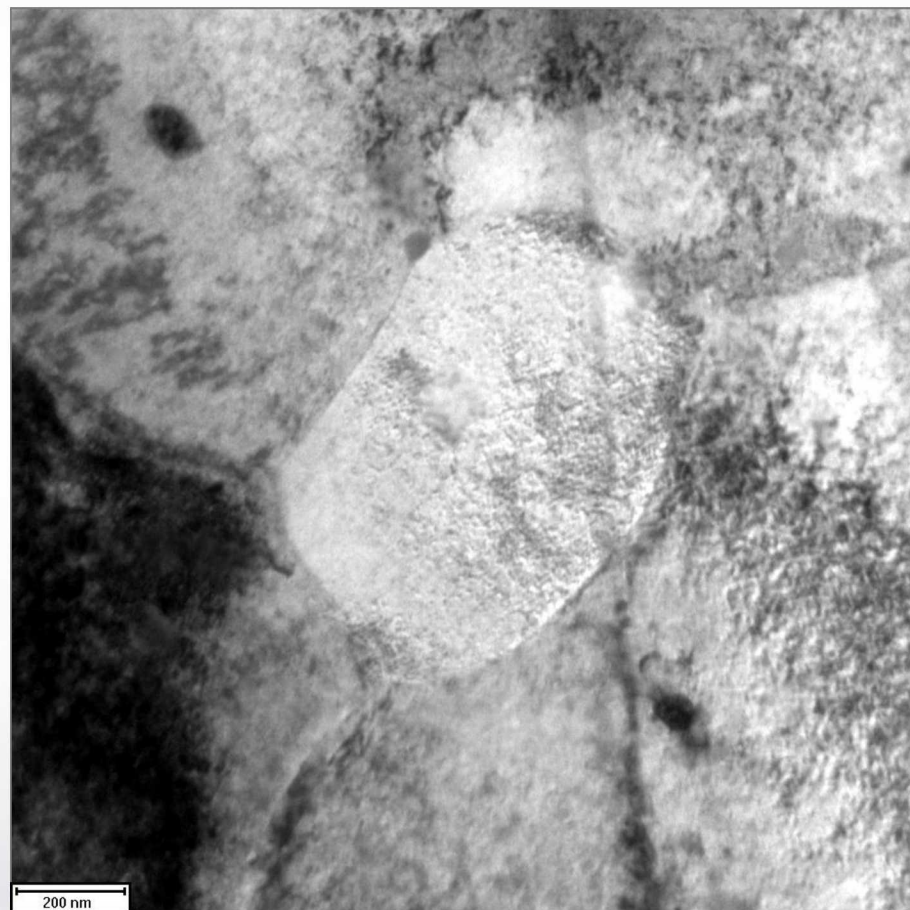
Two Beam  
g = 0002



# Concurrent He<sup>+</sup> Implantation and Self Ion Irradiation



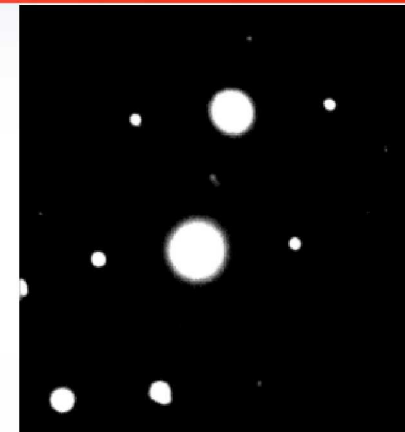
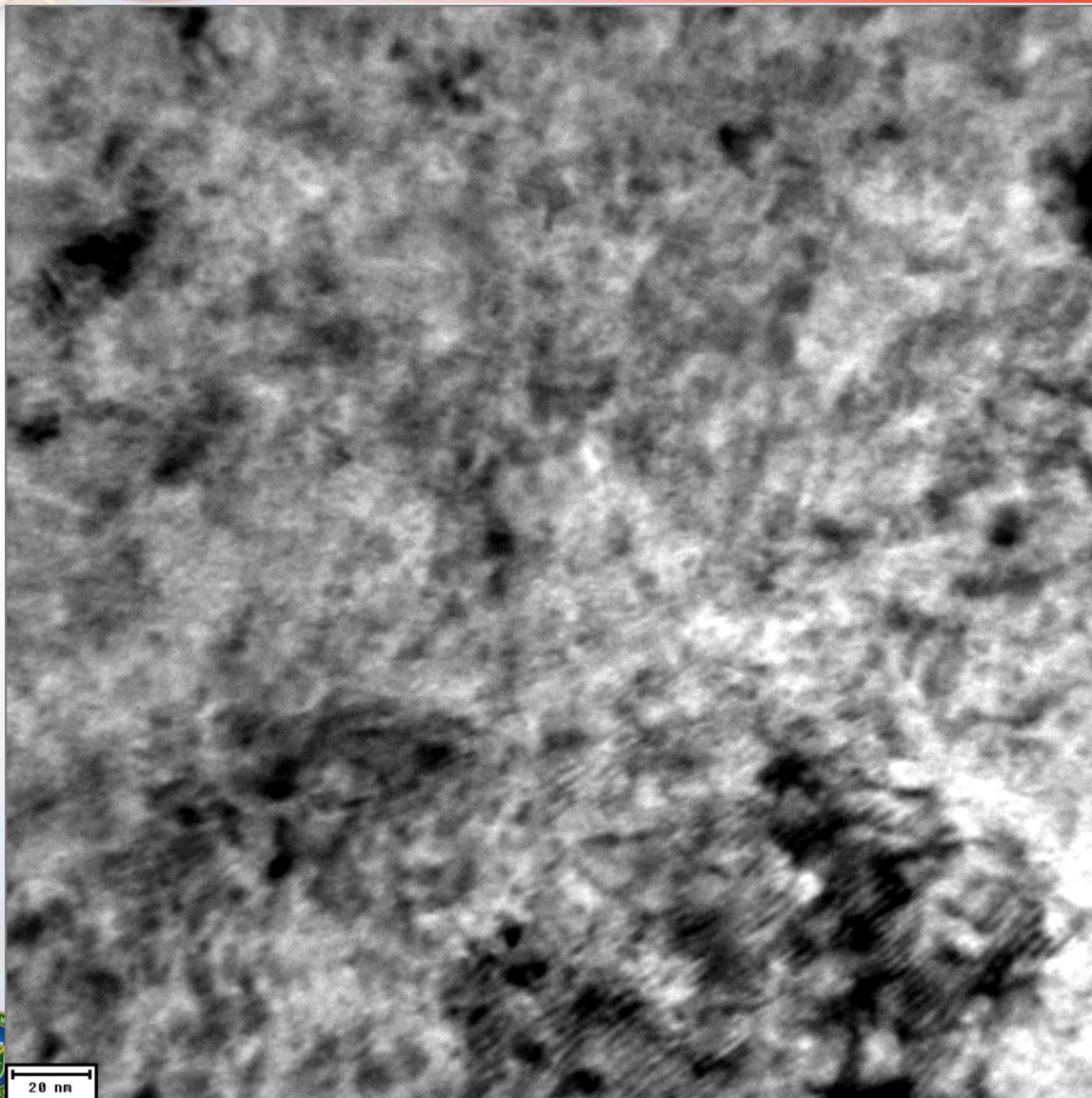
Before Implantation/Irradiation



After Implantation/Irradiation  
Damage, No Cavities



# Concurrent D & He Implantation & Zr Irradiation



Two Beam  
 $g = 1\bar{1}01$

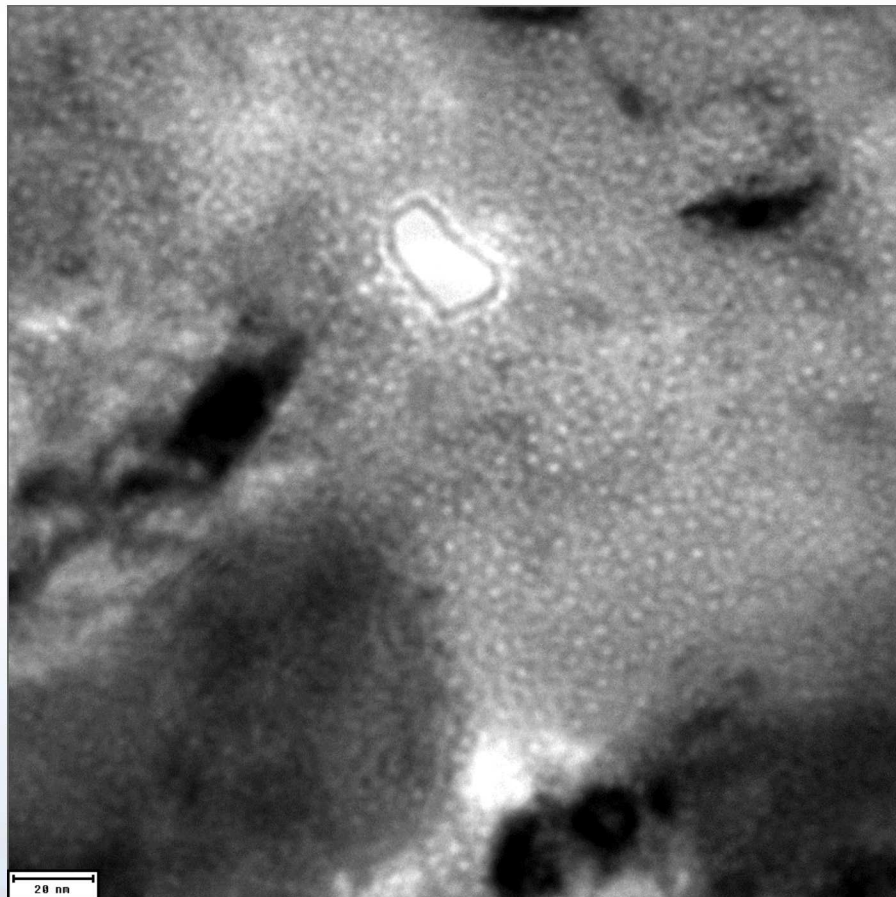


20 nm

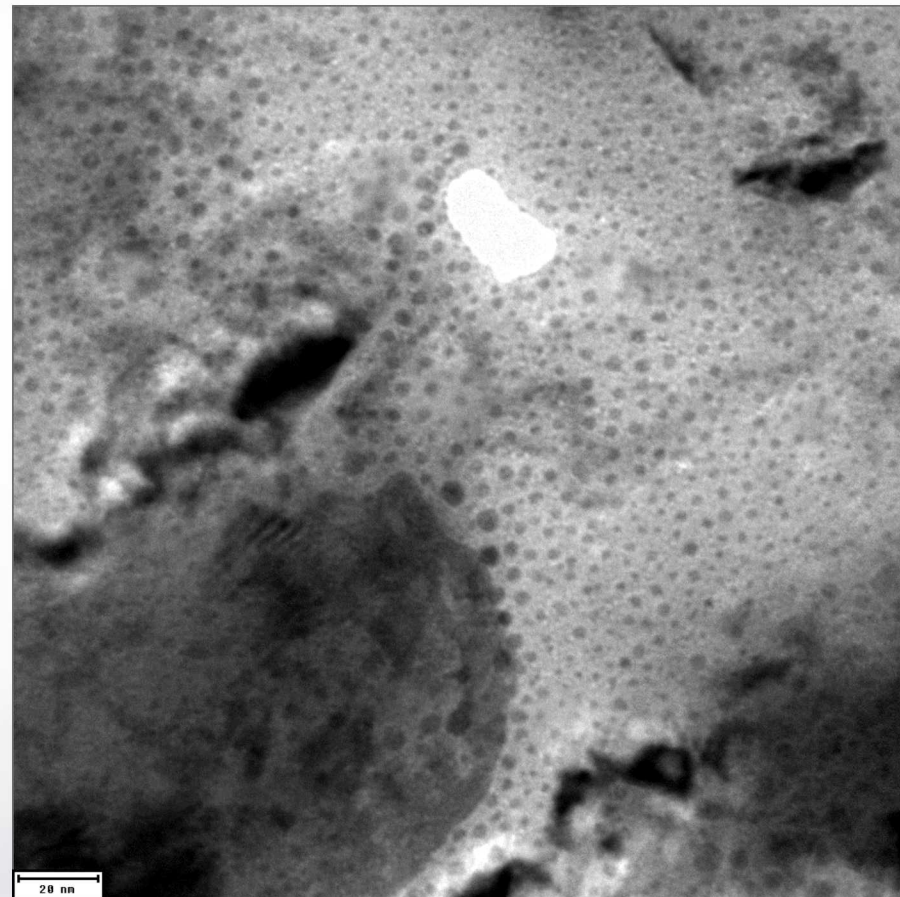


Sandia National Laboratories

# Through Focus Images: 30 Days Later



Under Focus

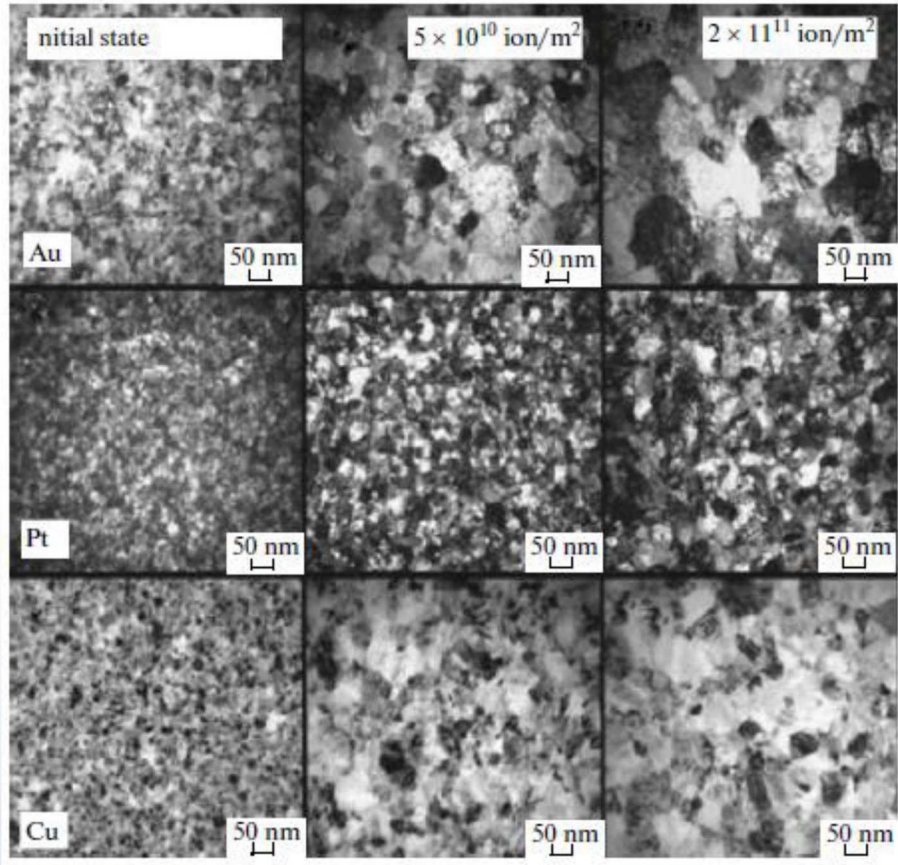


Over Focus



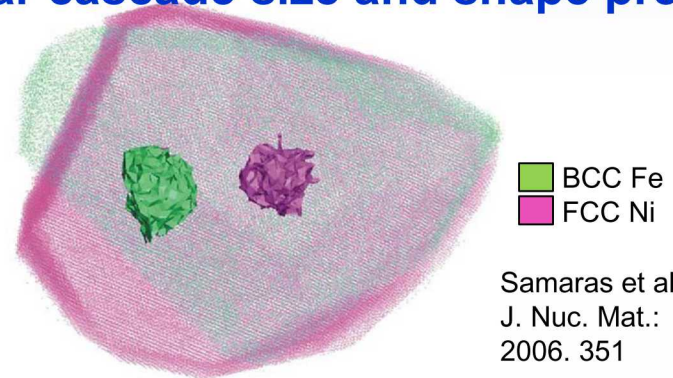
# Radiation Tolerance from Nanostructured Metals

## Variation in radiation tolerances



Kaomi et al., JAP: 2008. 104 073525

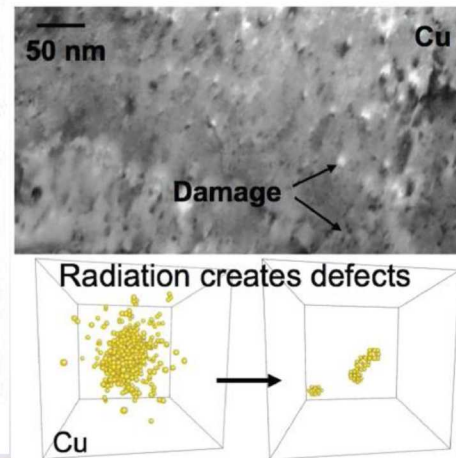
## Similar cascade size and shape predicted



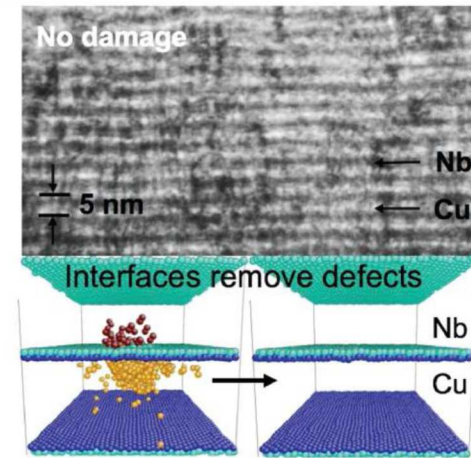
■ BCC Fe  
■ FCC Ni

Samaras et al.,  
J. Nuc. Mat.:  
2006. 351

## Nanolamellars are radiation tolerant



Demkowicz et al., MRS Bulletin: 2010. 35



To a first order mean grain size comparison, these reports appear conflicting.  
Not necessarily the case if initial microstructural details and associated properties are considered

# *In Situ* Irradiation

- Au foil during bombardment with 10 MeV Si<sup>3+</sup>
- ~22 s of 4000s total experiment time

Locations of single ion strikes and resulting microstructural change captured.



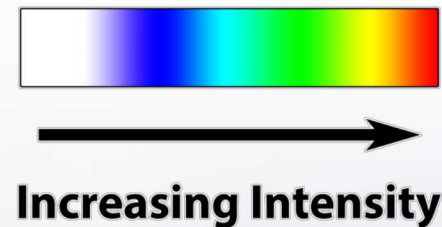
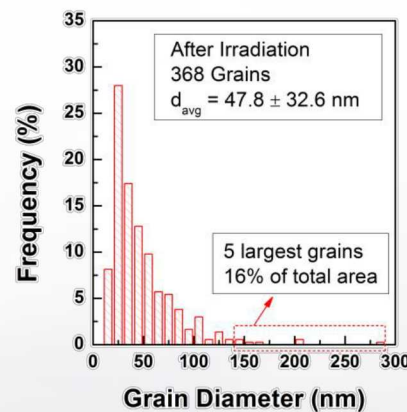
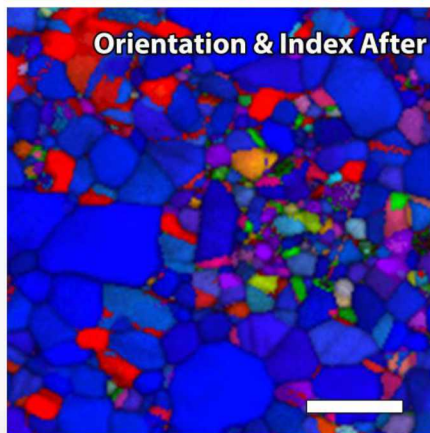
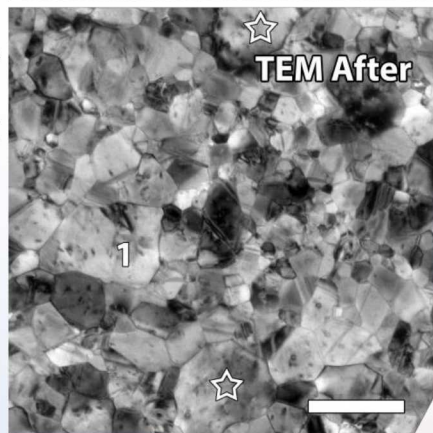
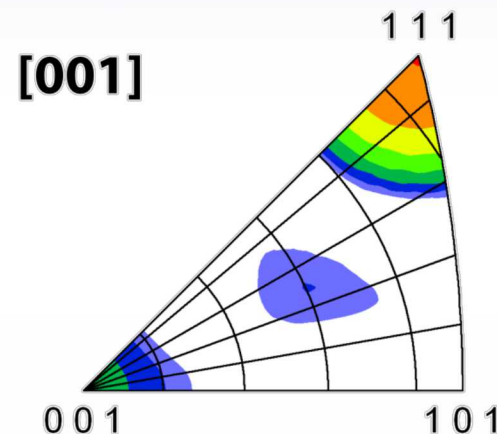
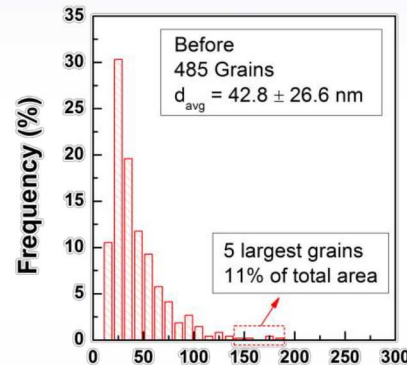
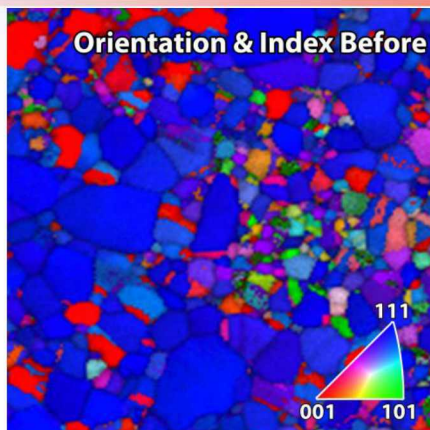
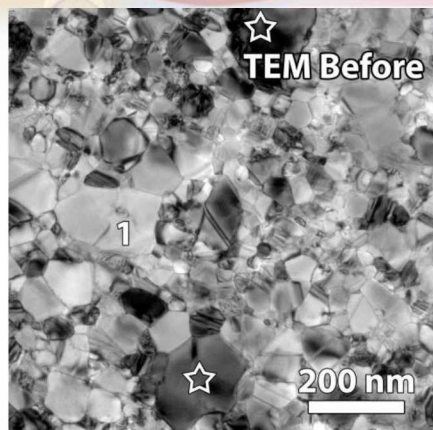
2 × real time

*In situ* ion irradiation  
TEM: 10 MeV Si into  
nanocrystalline Au.

Playback at 2 × real time.

# Quantification: Overall

Bufford, et al, J Appl Phys, 2015.



■ Same area characterized before and after irradiation.

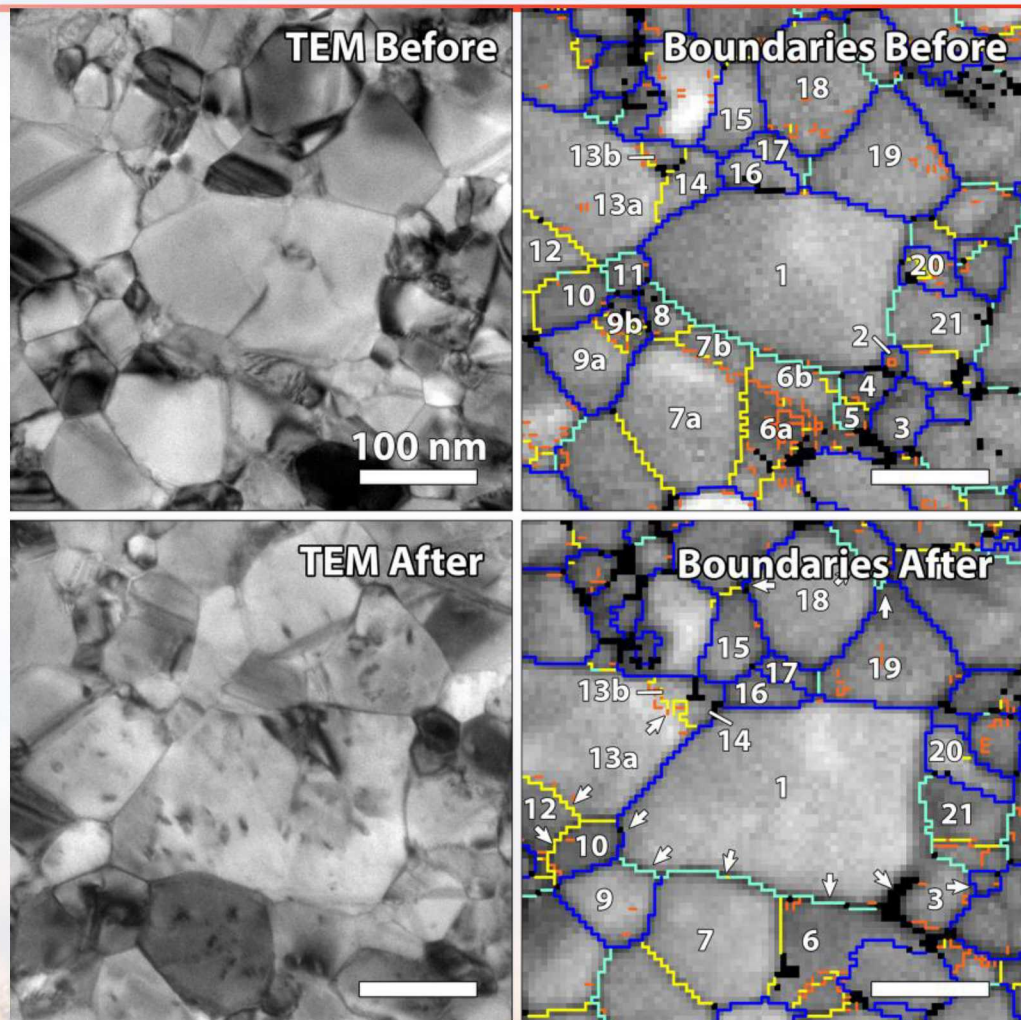
- Local grain size, orientation, boundary character
- Hundreds of grains counted in minutes

Rapid quantification of statistically relevant numbers of grains and boundaries.



# Quantification: Local

- The same grains identified before and after irradiation
- Individual grain boundary misorientation angles and axes quantified
- Correlation of GB properties and radiation-induced changes



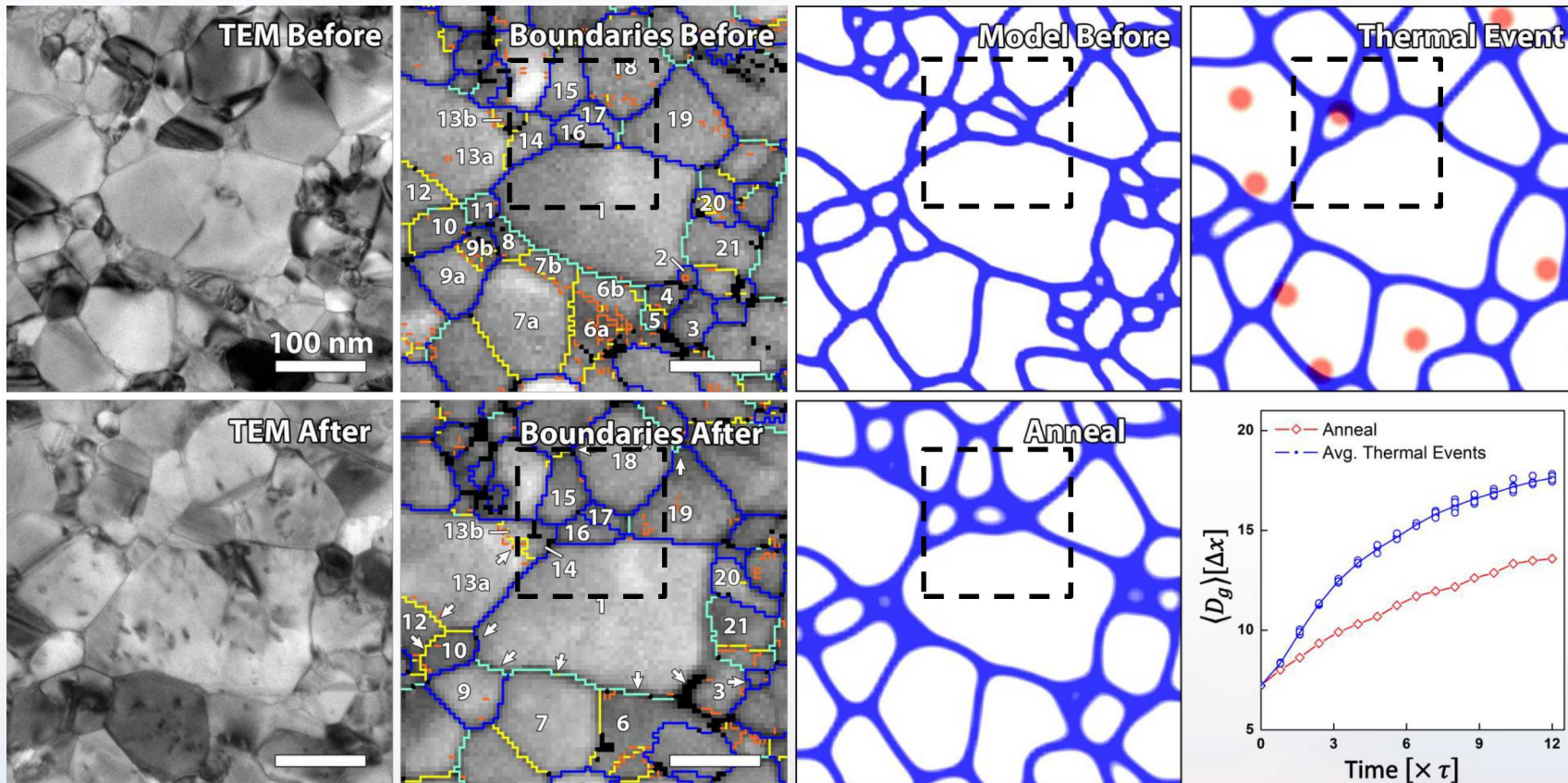
$3^\circ \leq \phi < 15^\circ$
$15^\circ \leq \phi < 30^\circ$
$30^\circ \leq \phi$

Individual grain boundary misorientation angle and axes quantified



# Exp. & Model Comparison

Bufford, et al, J Appl Phys, 2015.



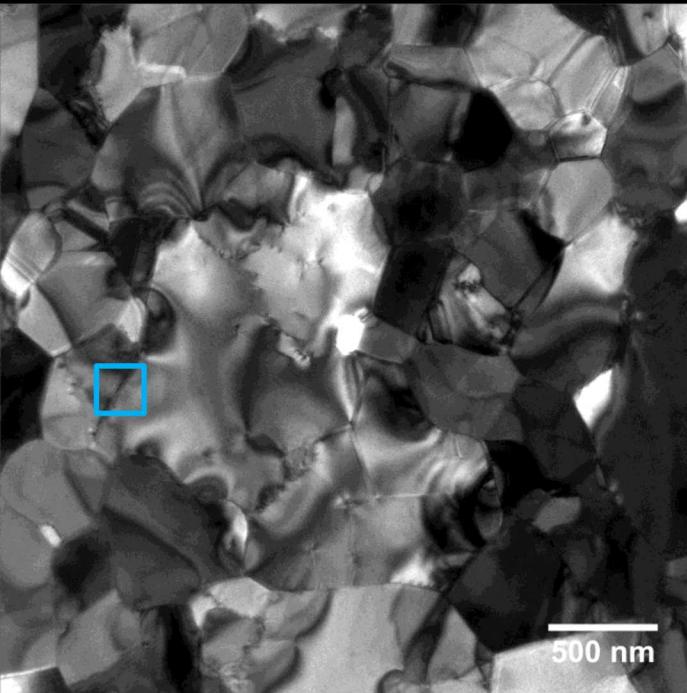
- Overall scaling laws appear consistent
- Subtle deviations from homogenous grain growth

Immobile boundaries suggest importance of non-thermally activated mobility



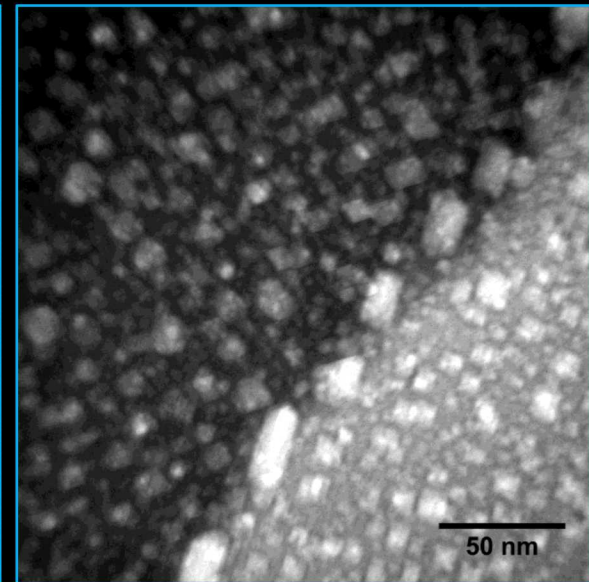
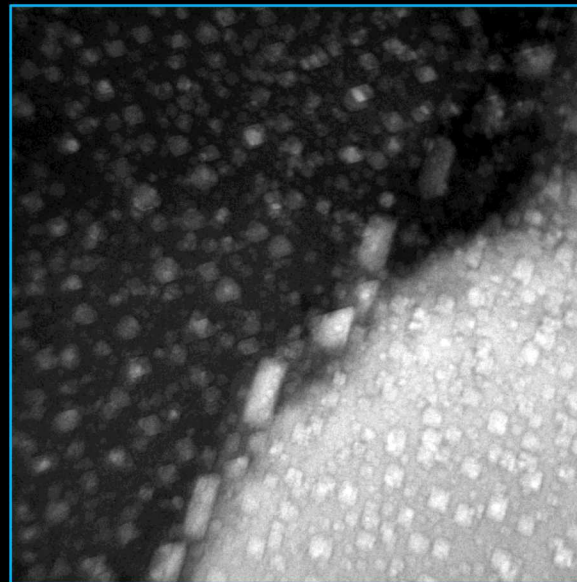
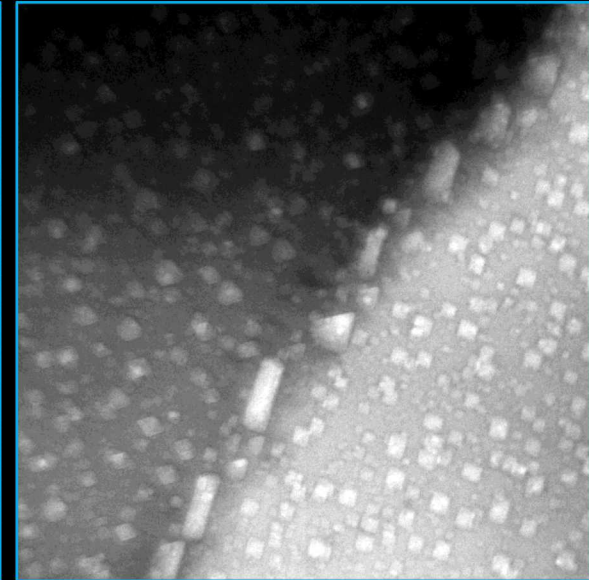
# *In situ* Implantation

Collaborators: C. Chisholm, P. Hosemann, & A. Minor



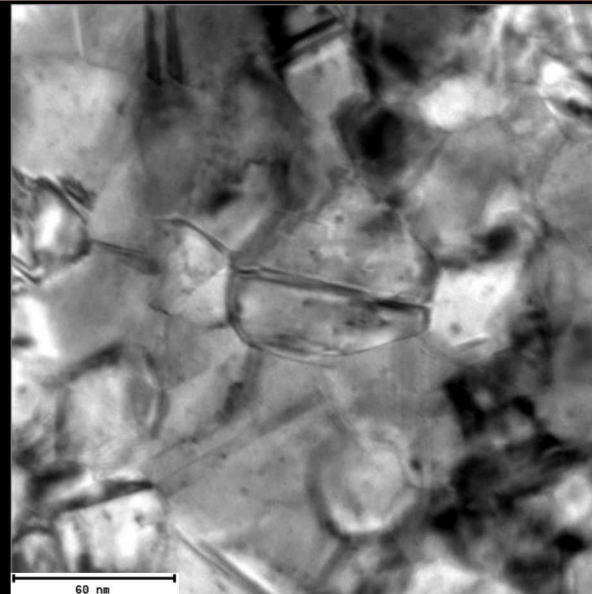
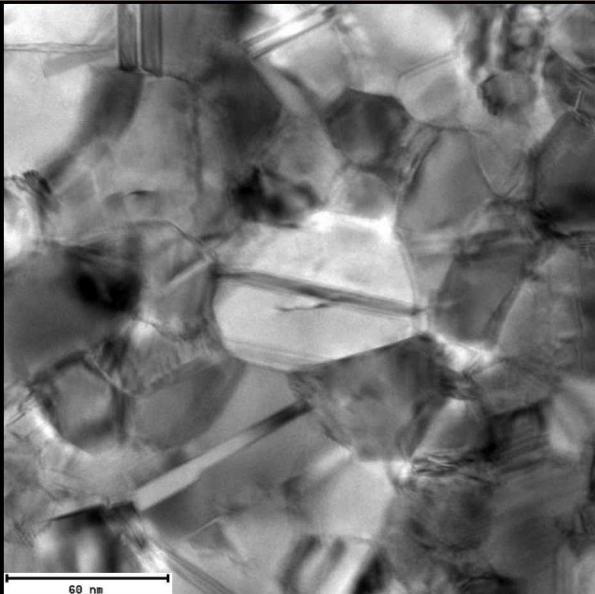
**Gold thin-film implanted  
with 10keV He<sup>2+</sup>**

**Result: porous  
microstructure**



# Nanocrystalline vs. Nanoporous Au results

Collaborators: N. Briot and T.J. Balk

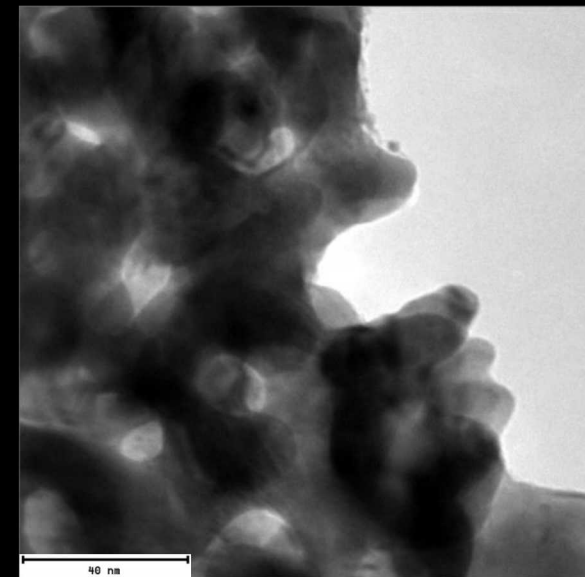
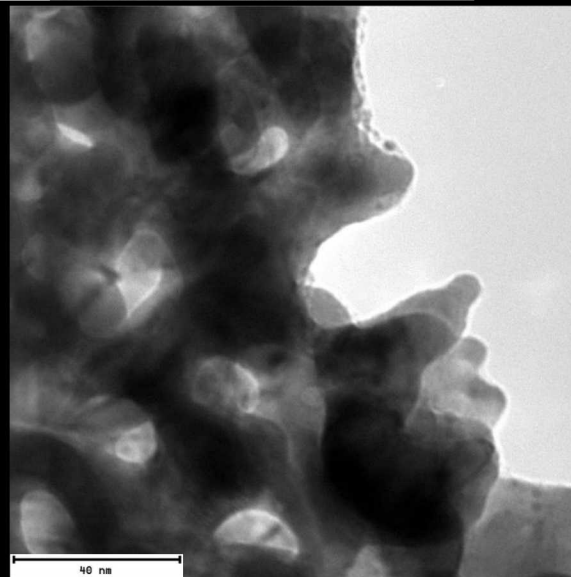


Nanoporous Au after ~ 6.6 dpa at  
46 keV:

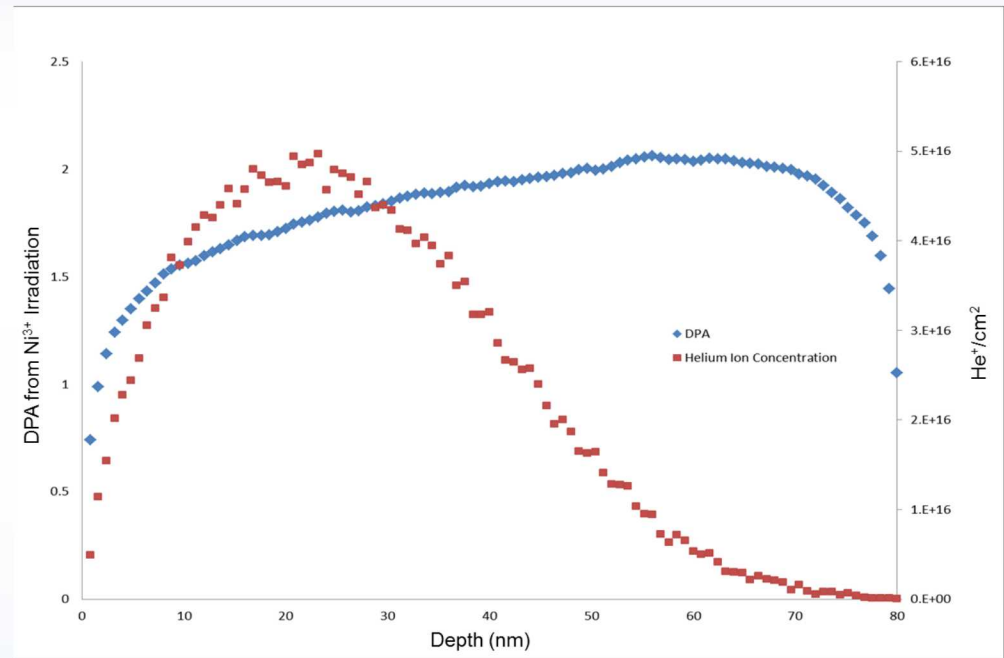
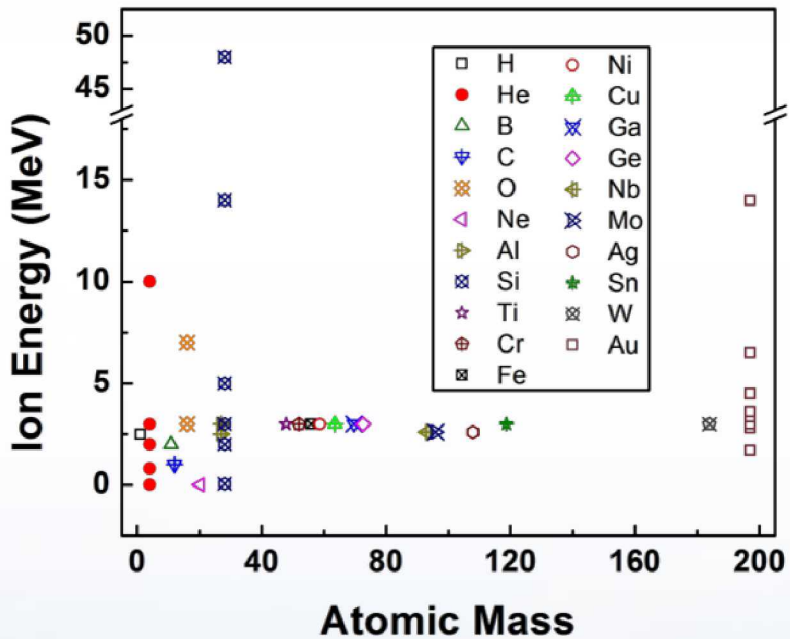
Melting of the ligament

Nanocrystalline Au after ~ 0.5 dpa  
at 46 keV:

Lots of defects constantly created



# Ion Beam Conditions



Order	Ni <sup>3+</sup> Rate	Ni <sup>3+</sup> damage	He Rate	He concentration
	ions/cm <sup>2</sup> s	DPA	ions/cm <sup>2</sup> s	ions/cm <sup>2</sup>
Ni <sup>3+</sup> , He <sup>+</sup>	1.5 E11	1.8	2.6 E 13	3 E 16
He <sup>+</sup> , Ni <sup>3+</sup>	1.5 E11	0.7	5.5 E13	1 E 17



# Irradiation / Implantation Sequence Effect on Cavity Structure

**Ni<sup>3+</sup> then He<sup>+</sup>**

**He<sup>+</sup> then Ni<sup>3+</sup>**

100 nm

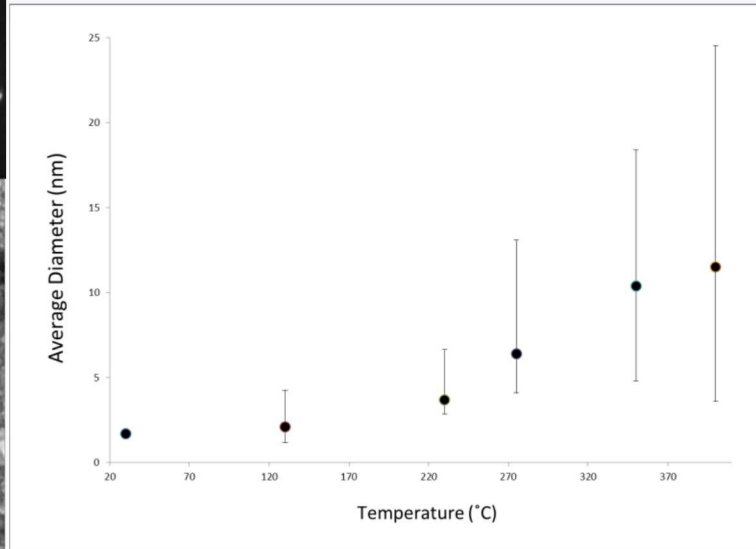
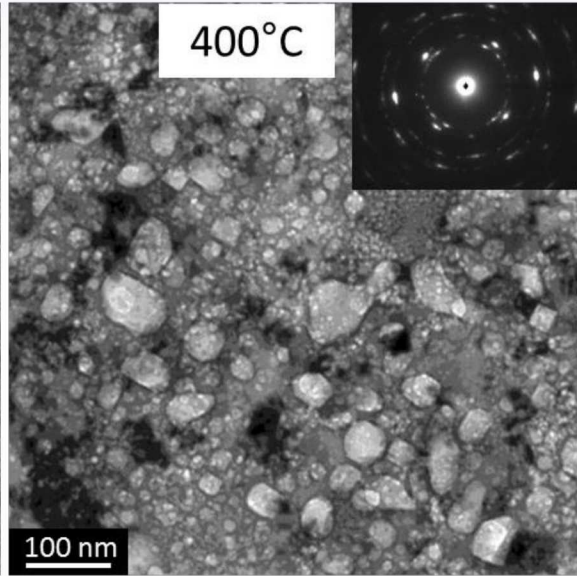
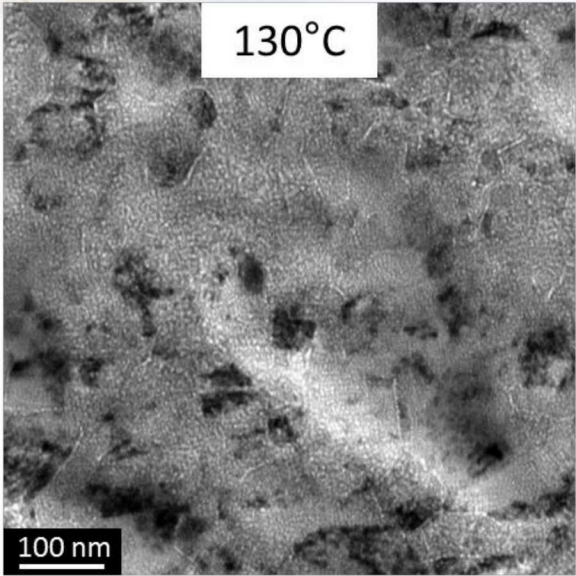
100 nm

Evenly distributed  
cavities over the entire  
grain structure

Apparent higher  
concentration of cavities  
along grain boundaries

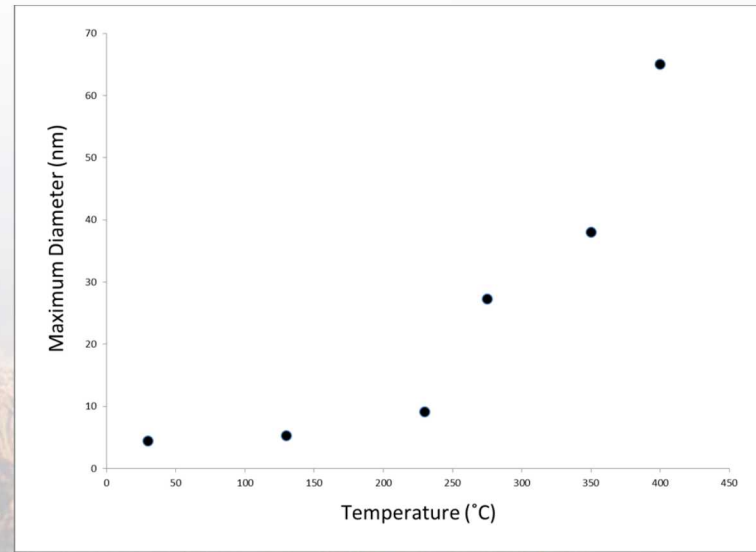
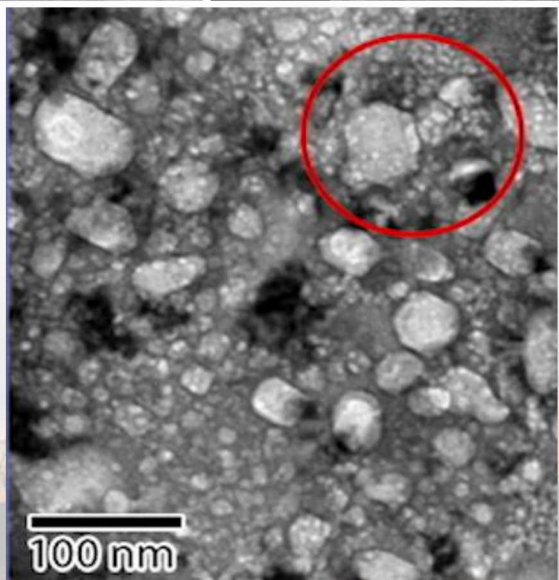


# Cavity Growth during In-situ Annealing of 10 keV He<sup>+</sup> Implanted and then 3 MeV Irradiated Ni<sup>3+</sup>



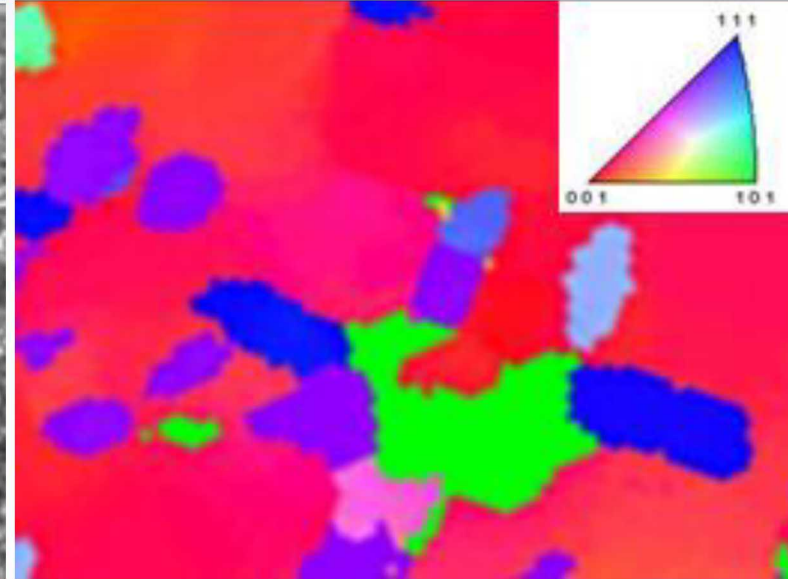
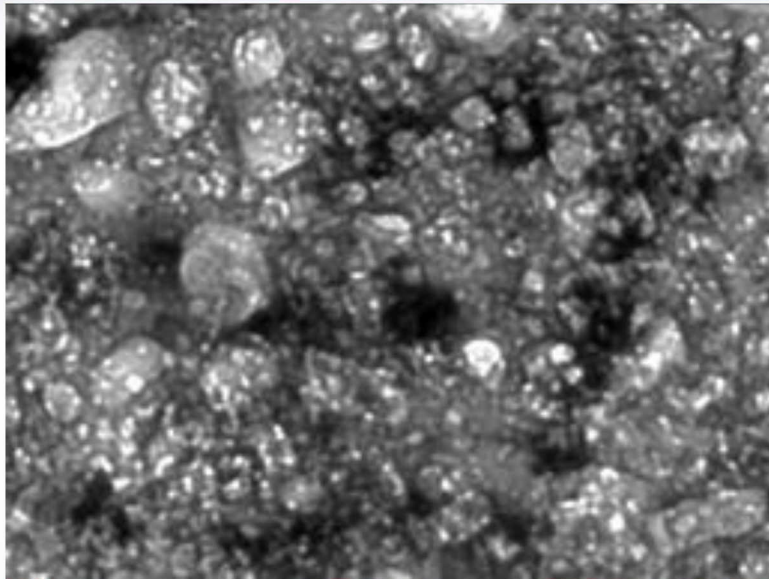
Bubble to cavity transition and cavity evolution can be directly studied

UNIVERSITY OF ARKANSAS  
FACULTY OF ENGINEERING  
STATE COLLEGE, ARKANSAS

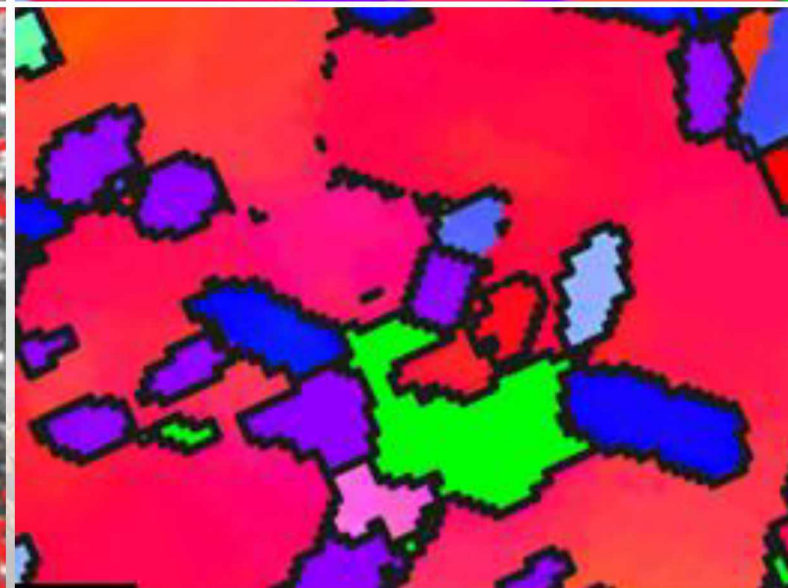
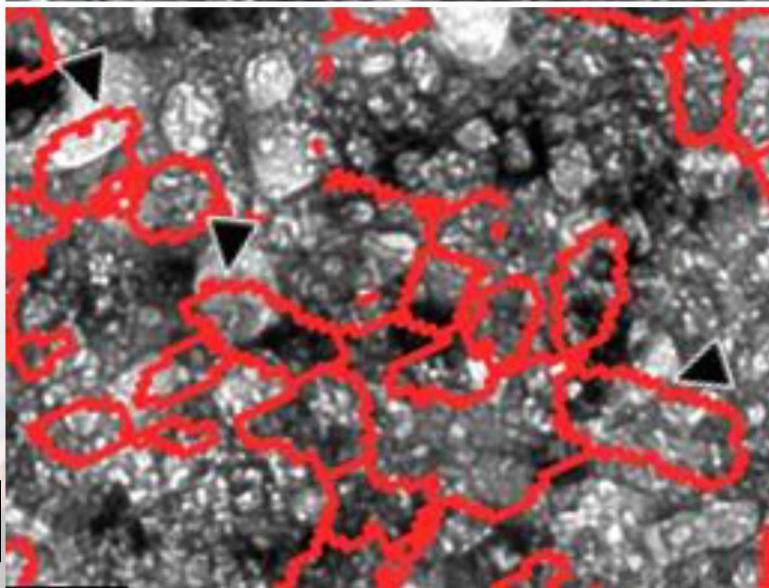


# Precession Electron Diffraction Reveals Hidden Grain Structure

Cavities in helium implanted, self-ion irradiated, nc nickel film annealed to 400 °C



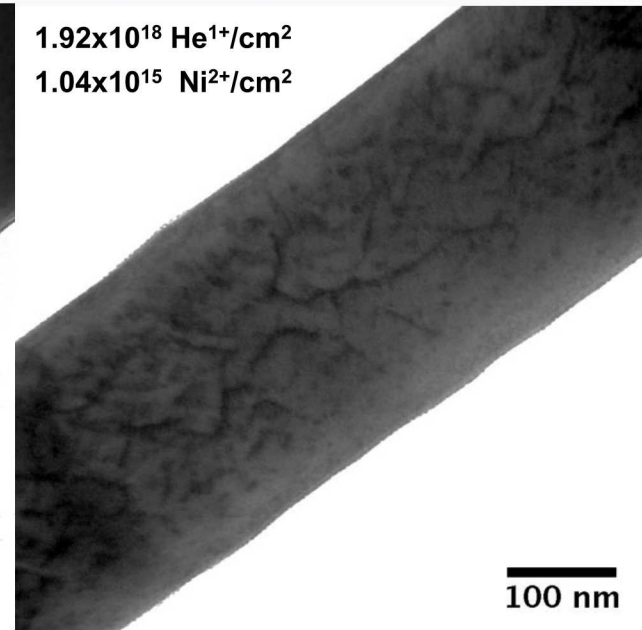
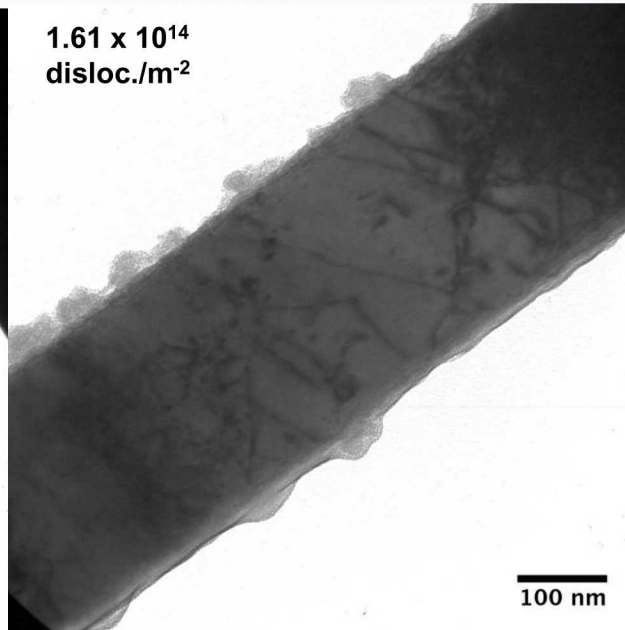
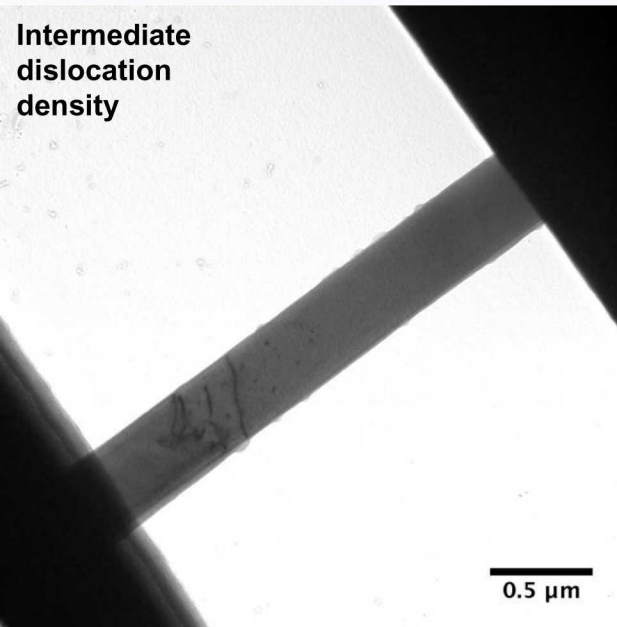
Cavities span multiple grains at identified grain boundaries



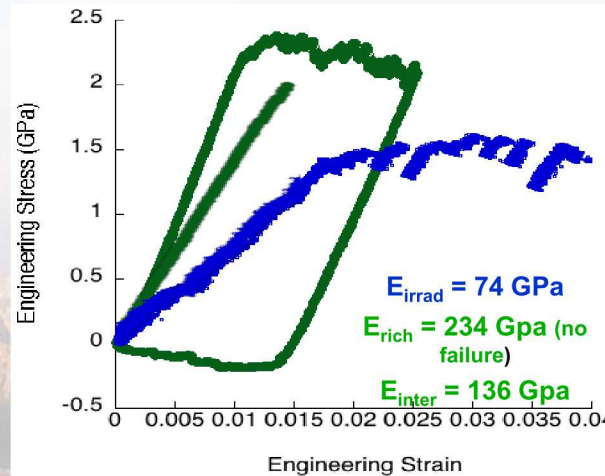
100 nm

# Next Steps: *In situ* TEM Quantitative Mechanical Testing

Contributors: C. Chisholm, H. Bei, E.P. George, P. Hosemann, & A.M. Minor



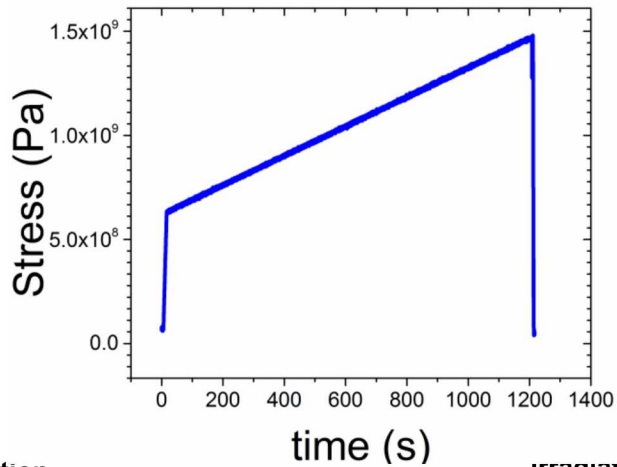
Work has started by looking sequentially at the quantitative effects of ion irradiation on mechanical properties utilizing in-situ ion irradiation TEM and in-situ TEM straining.



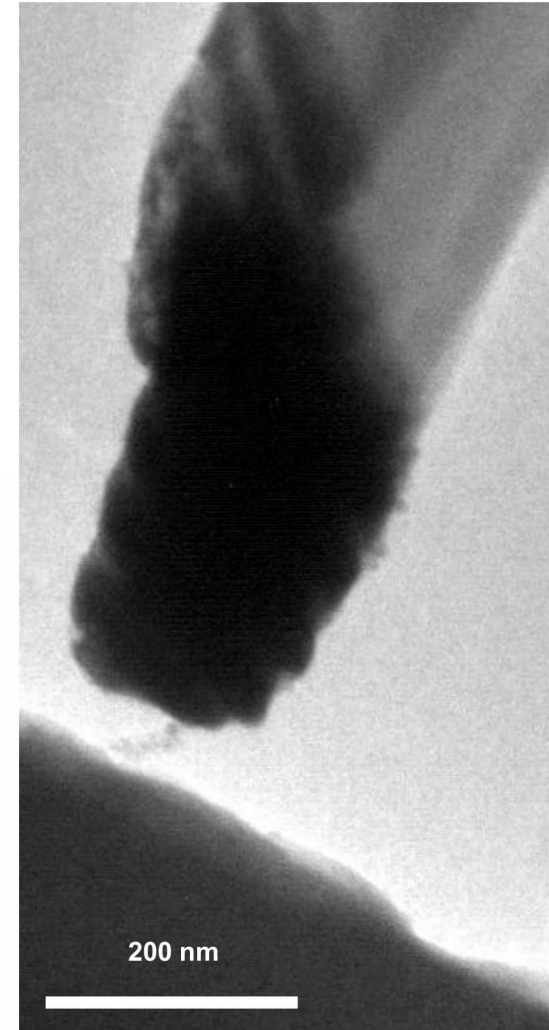
Sandia National Laboratories

# Irradiation Creep (4 MeV Cu<sup>3+</sup> 10<sup>-2</sup> DPA/s)

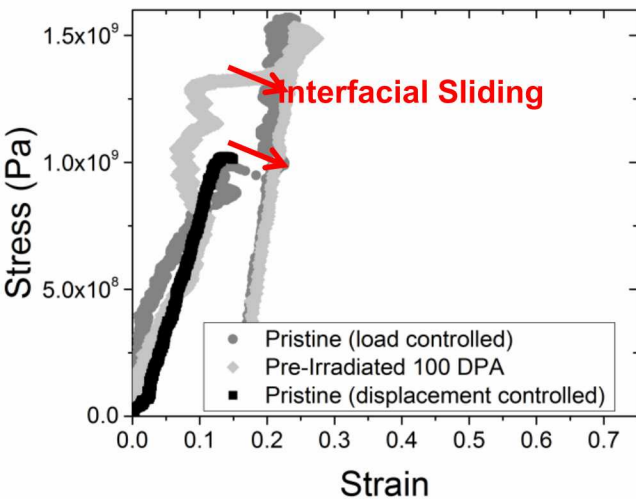
Controlled Loading Rate Experiments



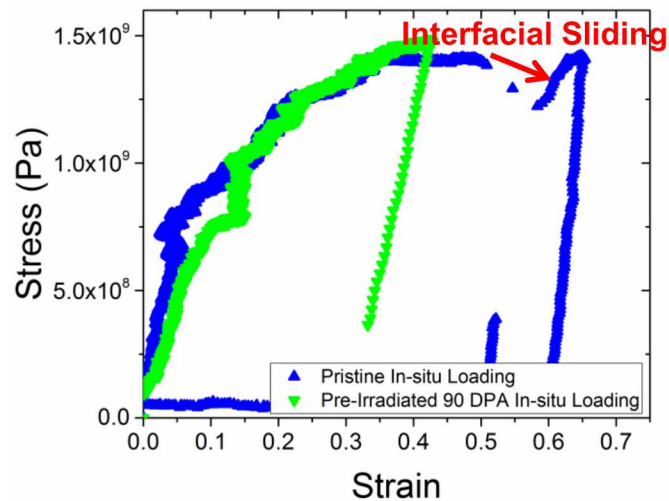
50 nm Cu-W multilayer  
20 Min



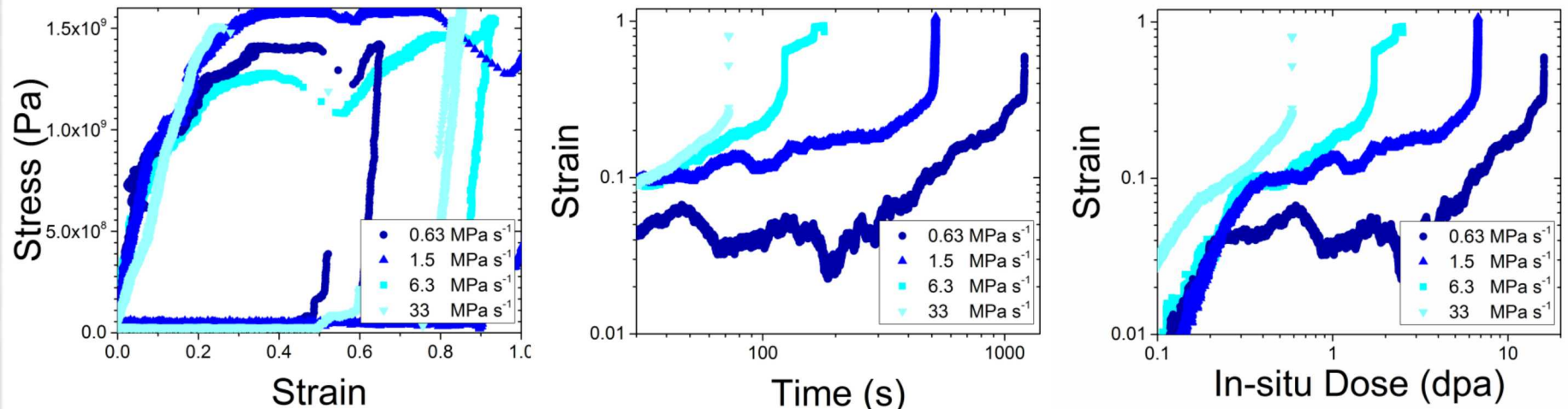
No Irradiation  
(Loading rate 0.6 Mpa s<sup>-1</sup>)



Irradiation Creep  
(Loading rate 0.6 Mpa s<sup>-1</sup>)



# Creep Response at Different Loading Rates

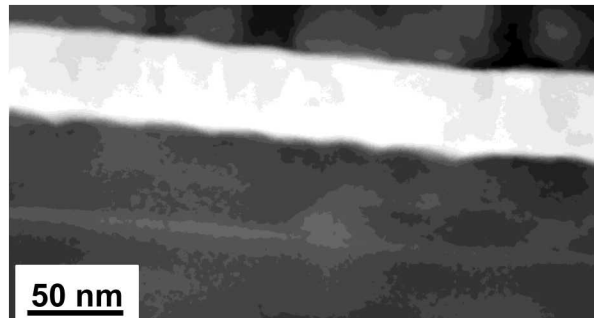


*Significant creep observed at a fraction of the bulk yield strength*

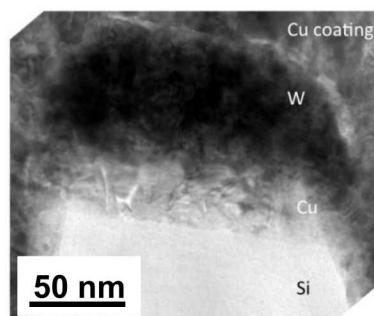
As-deposited Sample

Post Creep Characterization

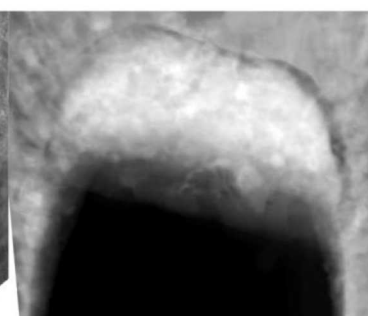
ADF-STEM



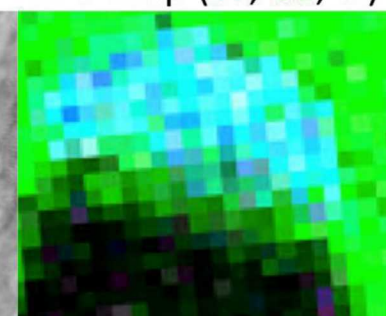
BF-TEM



ADF-STEM

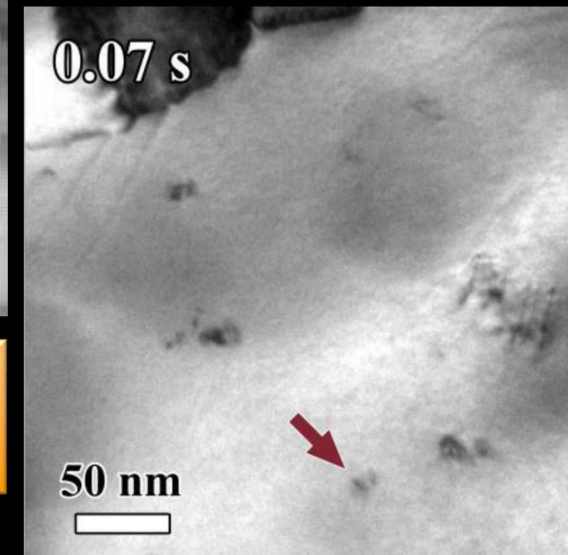
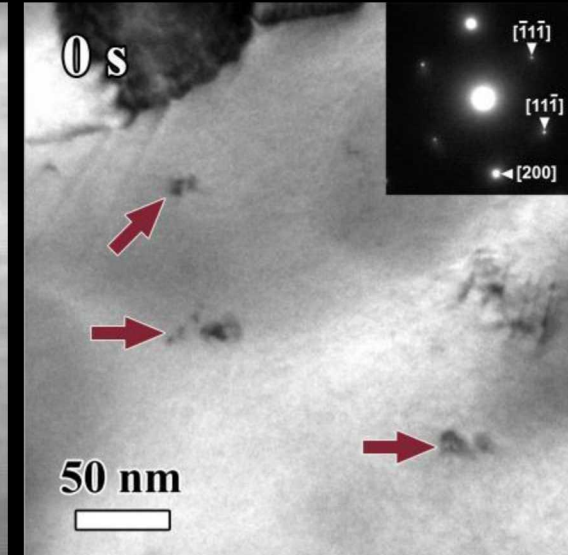


EDS Map (W, Cu, Si)



*Compression (creep) only observed in Cu layer*

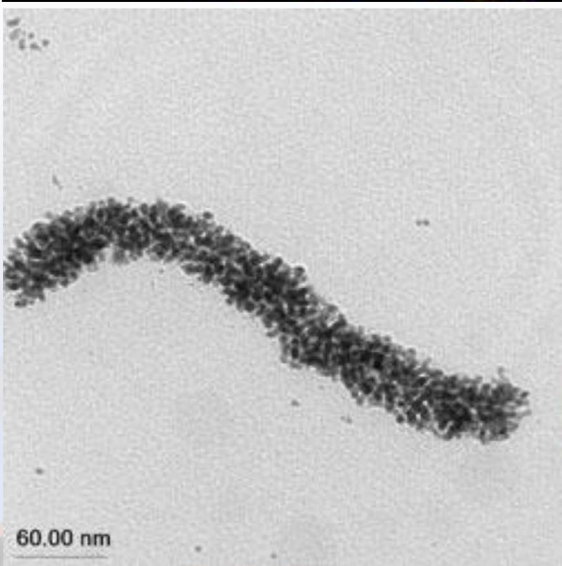
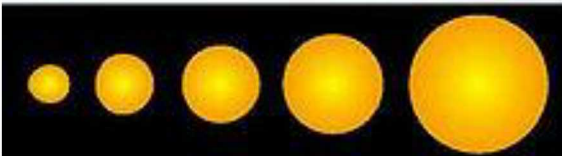
# 48 MeV Si into Au Thin Foil



Sped up 8x

The majority of expected Si ion strikes are not observed. Those observed result in significantly smaller defect structures.

# Nanoparticles in Extreme Environments

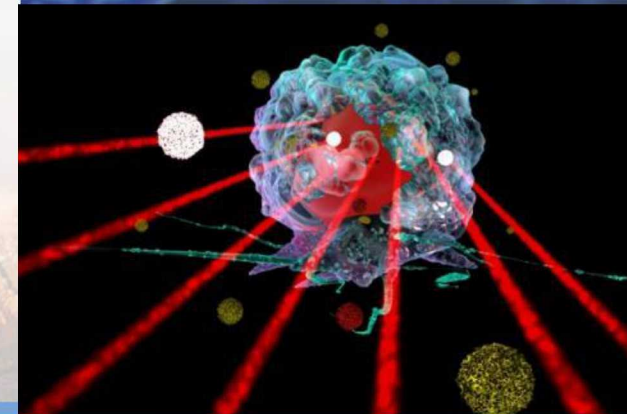
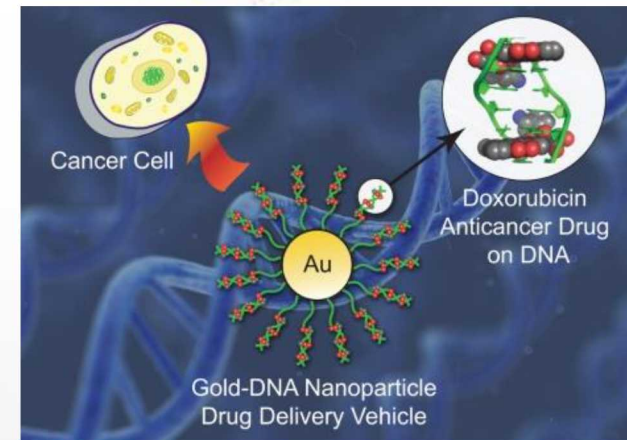


Nenoff et. al. *SNL News Release* (2007).

Au nanoparticles (Au NP) are of interest due to their unique optical, electronic, molecular-recognition, and catalytic properties

- Photothermal and laser ablation cancer therapies – concentrate IR into heat
- Tumor targeting and drug carriers – enhance dose delivery
- Catalysts for air-pollution control

Do the unique properties of the NP withstand extreme radiation?



# Cumulative Effects of Ion Irradiation as a Function of Ion Energy and Au Particle Size

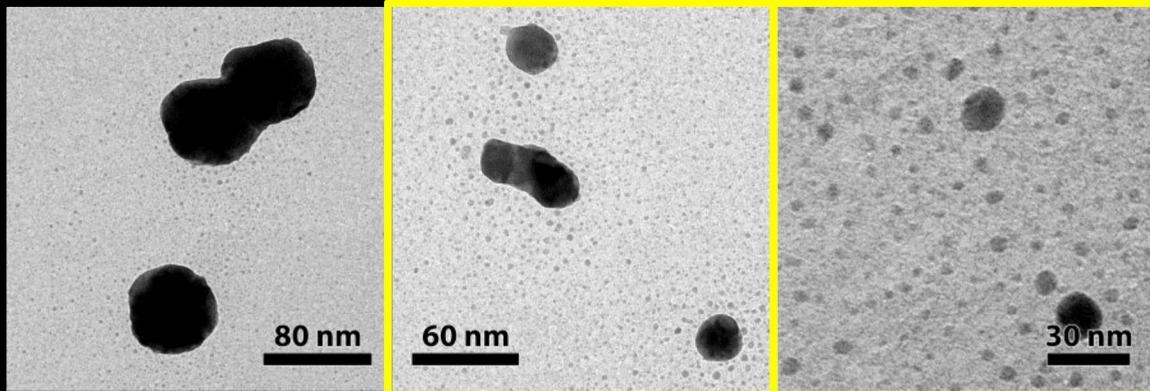
60 nm

20 nm

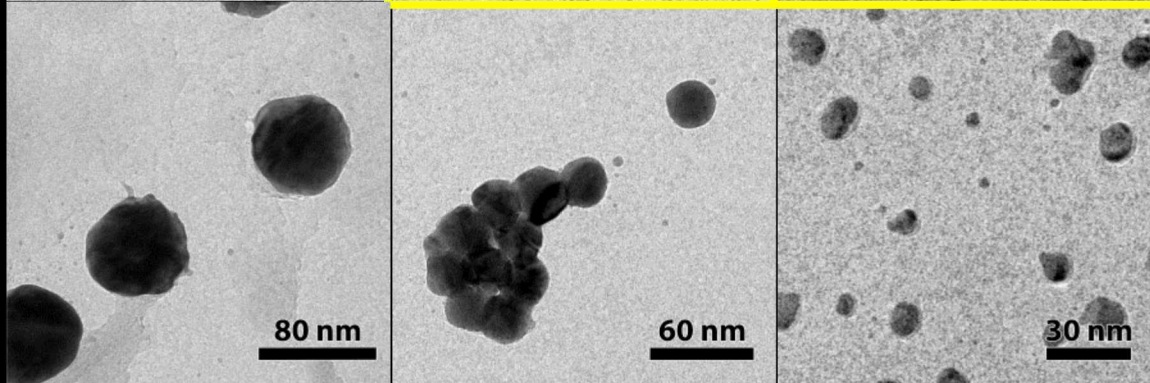
5 nm

Collaborator: D.C. Bufford

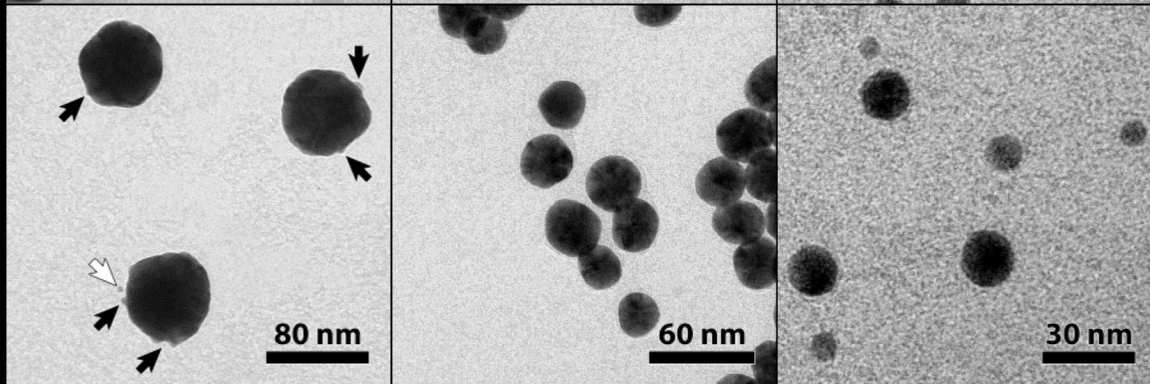
46 keV Au<sup>1+</sup>  
 $3.4 \times 10^{14} / \text{cm}^2$



2.8 MeV Au<sup>4+</sup>  
 $4 \times 10^{13} / \text{cm}^2$



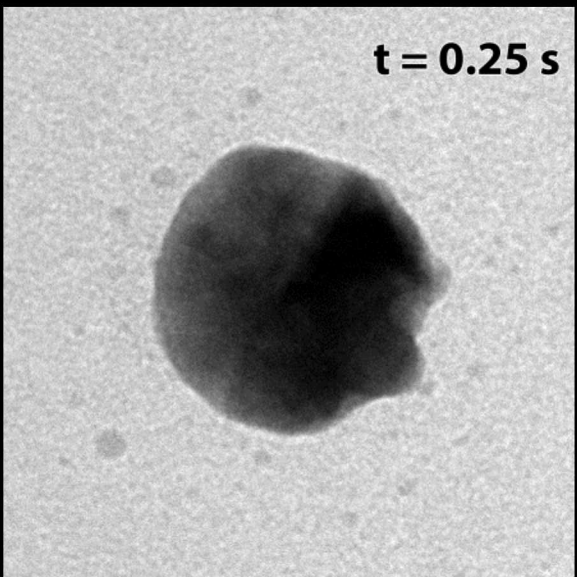
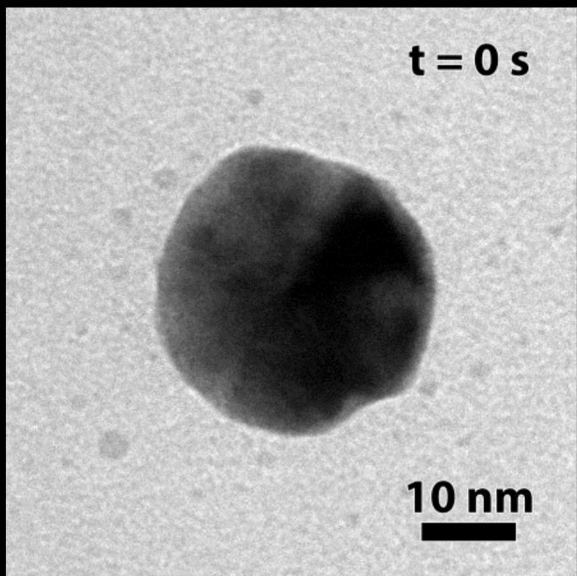
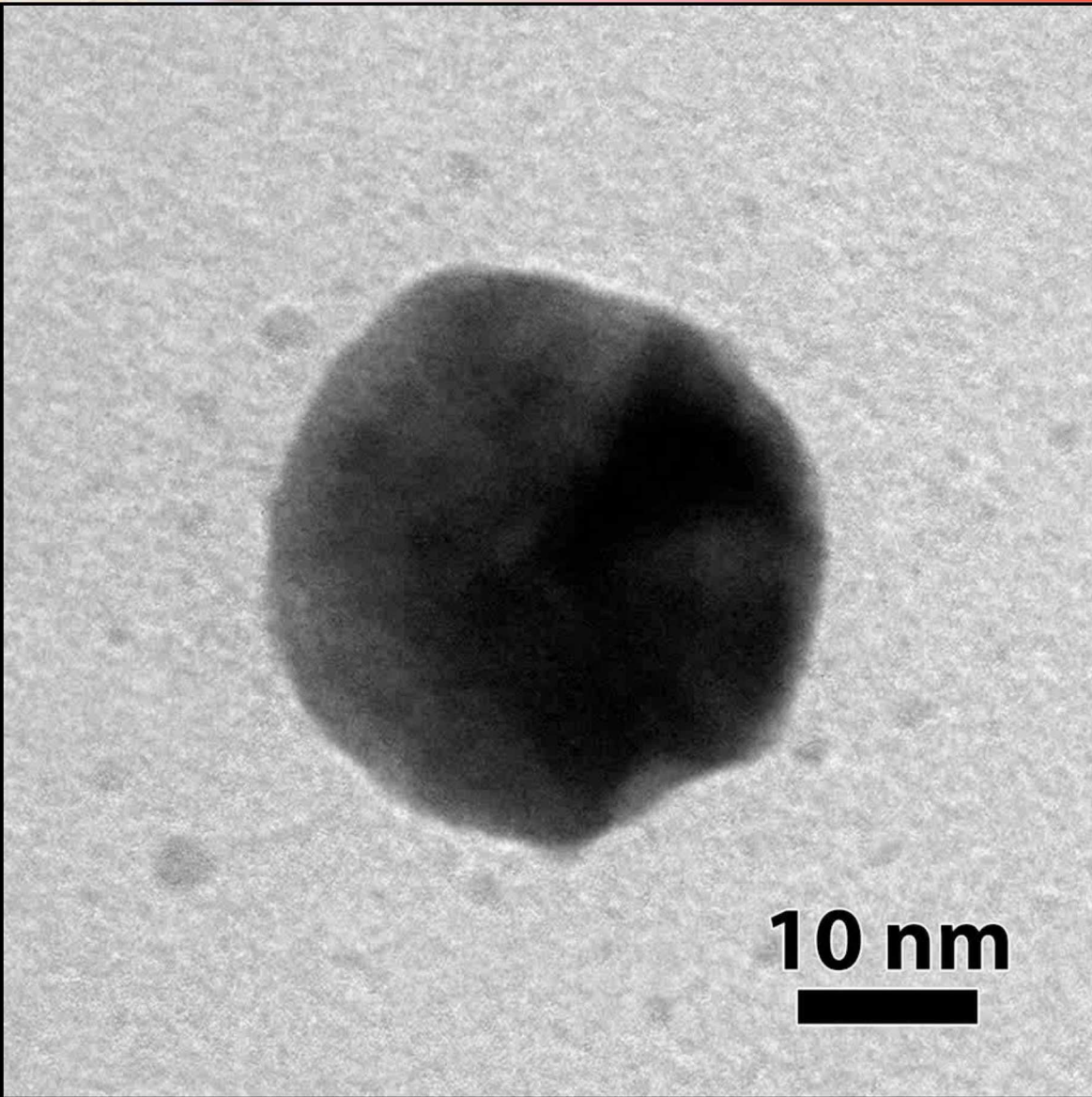
10 MeV Au<sup>8+</sup>  
 $1.3 \times 10^{12} / \text{cm}^2$



Particle and ion energy dictate the ratio of sputtering, particle motion, particle agglomeration, and other active mechanisms

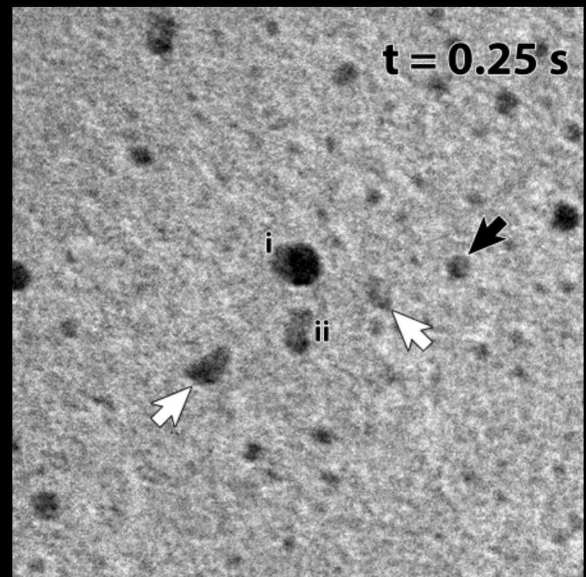
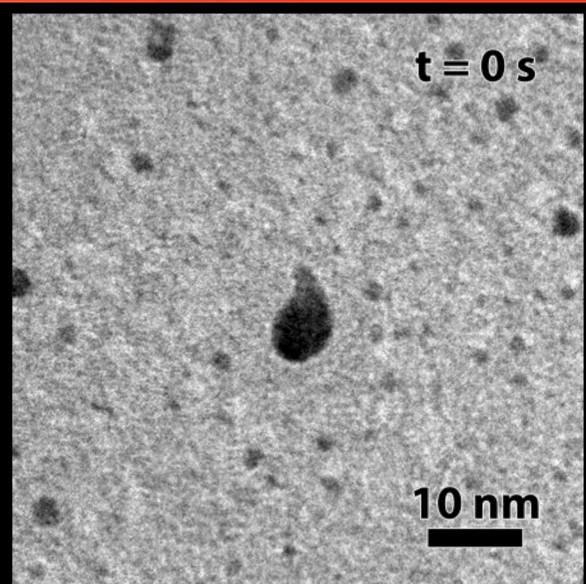
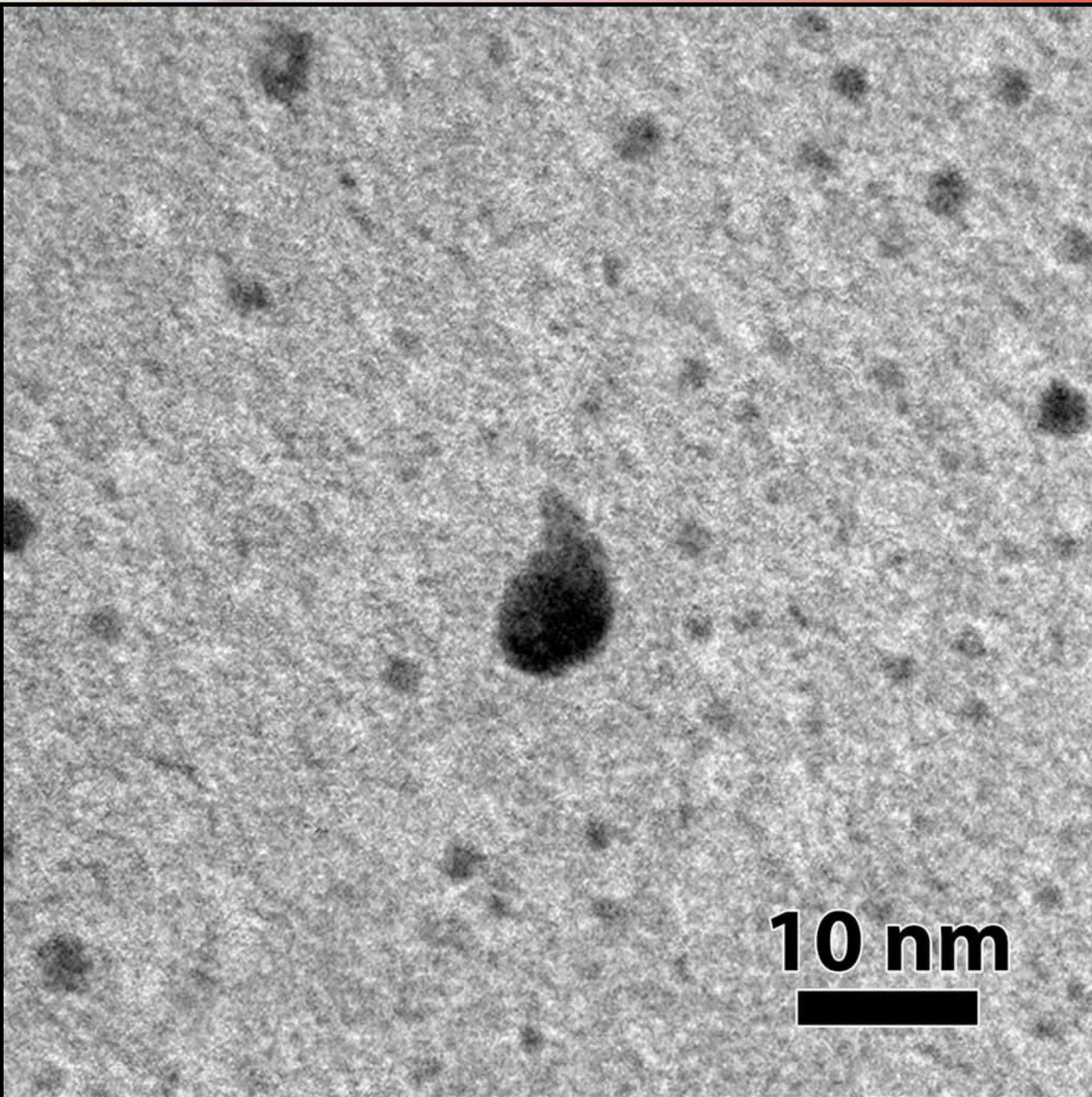
# Single Ion Effects with 46 keV Au<sup>1+</sup> ions: 20 nm

Collaborator: D.C. Bufford



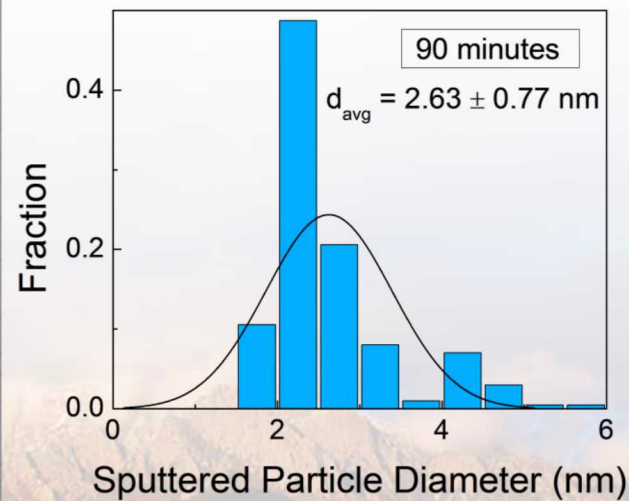
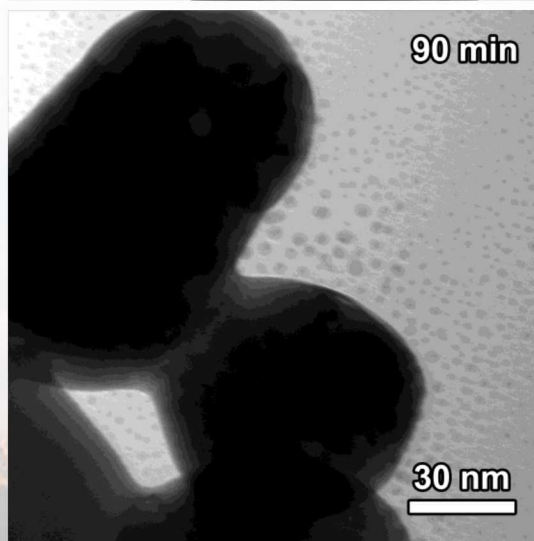
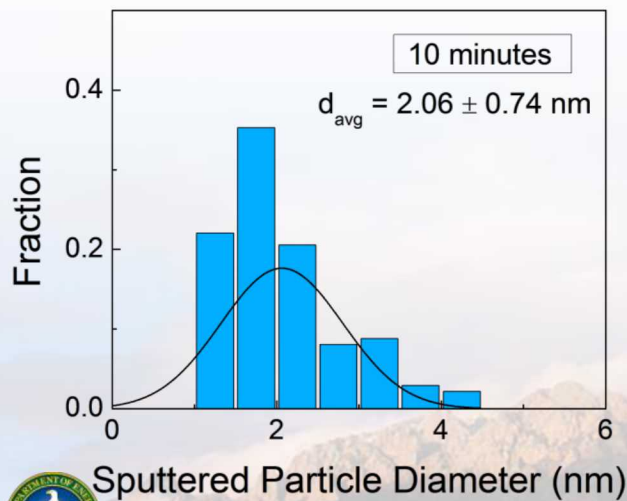
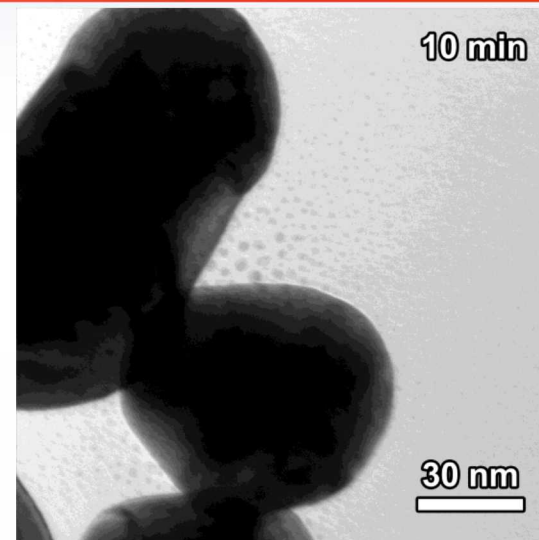
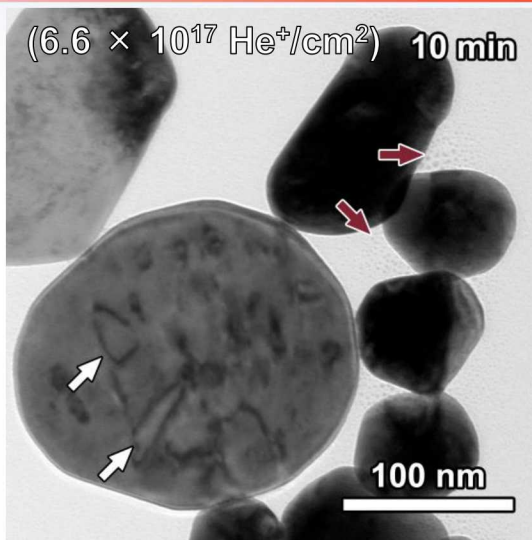
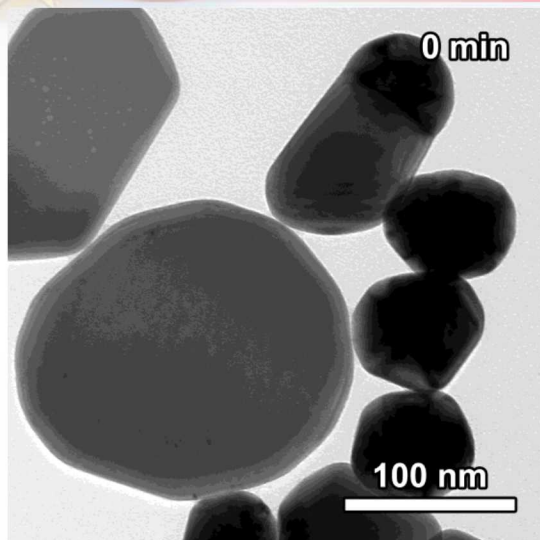
# Single Ion Effects with 46 keV Au<sup>1+</sup> ions: 5 nm

Collaborator: D.C. Bufford



# Formation of Dislocation Loops & Sputtered Particles due to He implantation

Collaborators: D.C. Bufford, S.H. Pratt & T.J. Boyle



# Advanced Microscopy Techniques Applied to Nanoparticles in Radiation Environments

Collaborators: S.H. Pratt & T.J. Boyle

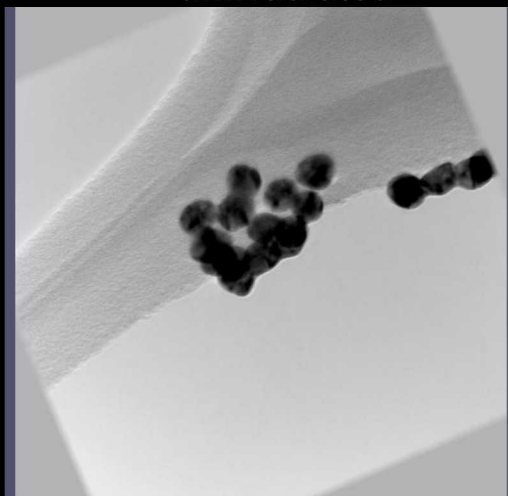
*In situ* Ion Irradiation TEM (I<sup>3</sup>TEM)

Aligned Au NP tilt series -  
unirradiated

Unirradiated Au NP model



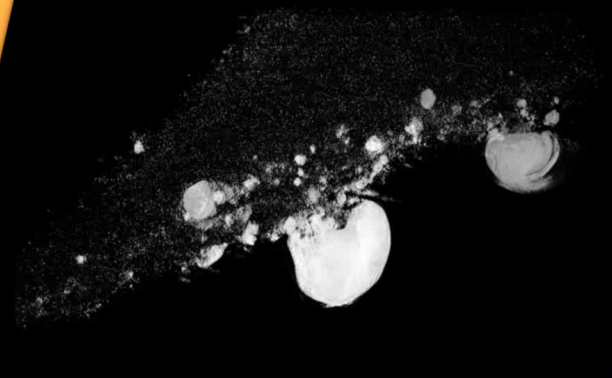
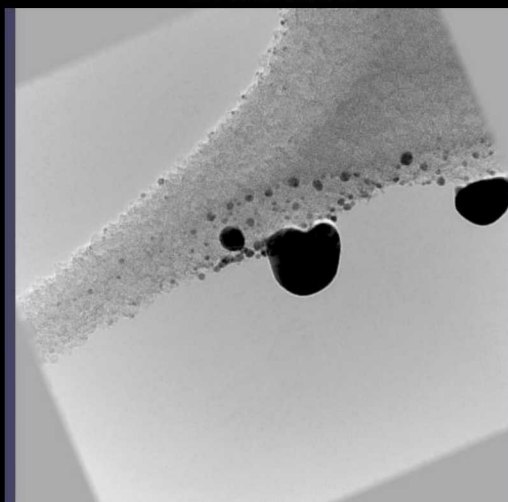
Hummingbird  
tomography stage



Aligned Au NP tilt series -  
irradiated



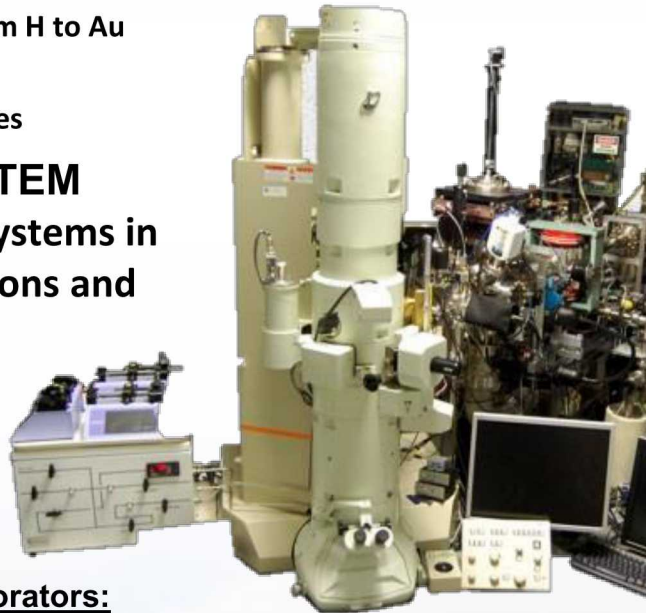
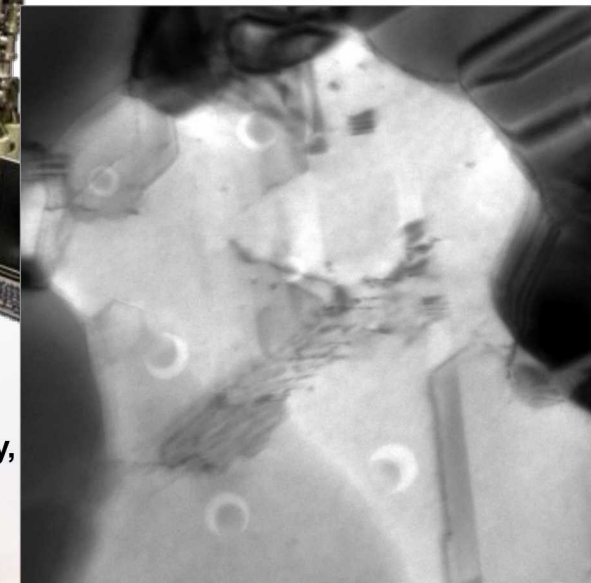
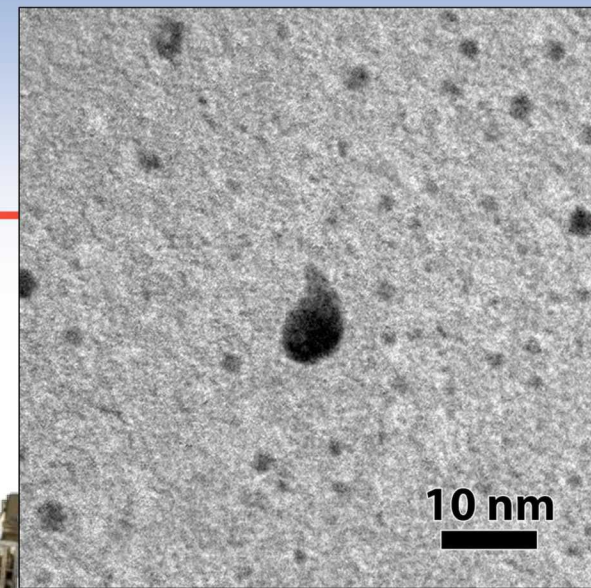
Irradiated Au NP model



The application of advanced  
microscopy techniques to  
extreme environments provides  
exciting new research directions

# Summary

- Sandia's I<sup>3</sup>TEM is one of only two facilities in the US
  - Only facility in the world with a wealth of dual *in situ* ion irradiation capabilities
  - *In situ* high energy ion irradiation from H to Au
  - *In situ* gas implantation
  - 14 TEM stages with various capabilities
- Currently applying the current I<sup>3</sup>TEM capabilities to various material systems in combined environmental conditions and expand the capabilities



## Collaborators:

- IBL: D.C. Bufford, D. Buller, C. Chisholm, B.G. Clark, J. Villone, G. Vizkelethy, B.L. Doyle, S. H. Pratt, & M.T. Marshall
- Sandia: B. Boyce, T.J. Boyle, P.J. Cappillino, J.A. Scott, B.W. Jacobs, M.A. Hekmaty, D.B. Robinson, E. Carnes, J. Brinker, D. Sasaki, J.A. Sharon, T. Nenoff, W.M. Mook, P. Feng, F.P. Doty, B.A. Hernandez-Sanchez, P. Yang, J-E Mogonye, S.V. Prasad, P. Kotula, S. Howell, T. Ohta, & T. Beechem
- External: A. Minor, L.R. Parent, I. Arslan, H. Bei, E.P. George, P. Hosemann, D. Gross, J. Kacher, & I.M. Robertson



This work was partially funded by the Division of Materials Science and Engineering, Office of Basic Energy Sciences, U.S. Department of Energy. Sandia National Laboratories is a multi-program laboratory managed and operated by Sandia Corporation, a wholly owned subsidiary of Lockheed Martin Corporation, for the U.S. Department of Energy's National Nuclear Security Administration under contract DE-AC04-94AL85000.



U.S. DEPARTMENT OF  
**ENERGY**

Office of  
Science



Sandia National Laboratories